



Calhoun: The NPS Institutional Archive
DSpace Repository

Theses and Dissertations

1. Thesis and Dissertation Collection, all items

1949

An analysis of precision methods of capacitance measurements at high frequency

Peale, William Trovillo

Annapolis, Maryland. U.S. Naval Postgraduate School

<http://hdl.handle.net/10945/31643>

This publication is a work of the U.S. Government as defined in Title 17, United States Code, Section 101. Copyright protection is not available for this work in the United States.

Downloaded from NPS Archive: Calhoun



<http://www.nps.edu/library>

Calhoun is the Naval Postgraduate School's public access digital repository for research materials and institutional publications created by the NPS community. Calhoun is named for Professor of Mathematics Guy K. Calhoun, NPS's first appointed -- and published -- scholarly author.

Dudley Knox Library / Naval Postgraduate School
411 Dyer Road / 1 University Circle
Monterey, California USA 93943

AN ANALYSIS OF PRECISION METHODS OF
CAPACITANCE MEASUREMENTS AT HIGH FREQUENCY

-
W. T. PEALE

Library
U. S. Naval Postgraduate School
Annapolis, Md.

AN ANALYSIS OF PRECISION METHODS OF
CAPACITANCE MEASUREMENTS AT HIGH FREQUENCY

by

William Trovillo Peale
Lieutenant, United States Navy


Submitted in partial fulfillment
of the requirements
for the degree of
MASTER OF SCIENCE
in
ENGINEERING ELECTRONICS

United States Naval Postgraduate School
Annapolis, Maryland
1949

This work is accepted as fulfilling ²¹
the thesis requirements for the degree of

MASTER OF SCIENCE
in
ENGINEERING ELECTRONICS

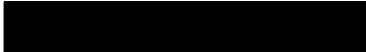
from the ⁸
United States Naval Postgraduate School


Chairman ¹⁰

Department of Electronics and Physics ⁵

Approved: ¹⁰

¹¹⁵²⁷


Academic Dean ⁴

PREFACE

The compilation of material for this paper was done at the General Radio Company, Cambridge, Massachusetts, during the winter term of the third year of the post-graduate Electronics course.

The writer wishes to take this opportunity to express his appreciation and gratitude for the cooperation extended by the entire Company and for the specific assistance rendered by Mr. Robert F. Field and Mr. Robert A. Soderman.

TABLE OF CONTENTS

LIST OF ILLUSTRATIONS

CHAPTER I: INTRODUCTION	1
1. Series Resonance Methods.	2
2. Parallel Resonance Methods.	4
3. Voltmeter-Ammeter Method.	7
4. Bridge Methods	8
5. The Twin-T Circuit.	10
CHAPTER II: THE CAPACITANCE STANDARD	14
CHAPTER III: THE RESISTANCE STANDARD	34
CHAPTER IV: SERIES RESONANCE METHODS	41
1. Substitution Method.	41
2. Resistance Variation Method.	45
3. Reactance Variation Method.	48
CHAPTER V: PARALLEL RESONANCE METHODS	51
1. Substitution Method.	51
2. Conductance Variation Method.	53
3. Susceptance Variation Method.	55
CHAPTER VI: THE VARIABLE DIODE CONDUCTANCE MEASURING CIRCUIT	57
CHAPTER VII: NULL METHODS	67
1. Impedance Bridge.	67
2. Modified Schering Bridge.	67
3. The 1601 VHF Bridge.	74
4. Twin-T Method.	80
CHAPTER VIII: CONCLUSIONS	87

BIBLIOGRAPHY

89

APPENDIX I

92

APPENDIX II

95

LIST OF ILLUSTRATIONS

Figure	TITLE	page
1.	Basis Circuit, Series Resonant Methods.	5
2.	Basic Circuit, Parallel Resonant Methods.	5
3.	Basic Q-Meter Circuit.	5
4.	Impedance Bridge-Basic Circuit.	9
5.	Modified Schering Bridge-Basic Circuit.	9
6.	Parallel-T Null Circuit.	13
7.	Stator Structure of Typical Precision Capacitor.	15
8.	Equivalent Circuit of Dissipationless, Precision Capacitor.	17
9.	Simplified Equivalent Circuit.	17
10.	Equivalent Circuit of Precision Capacitor.	20
11.	Simplified Equivalent Circuit of Precision Capacitor.	20
12.	Parallel Stray Capacitance.	23
13.	Plot for Determination of Residual Inductance of Precision Capacitor.	26
14.	Plot for Determination of Residual Resistance.	26
15.	Plot for Determination of Residual Conductance.	27
16.	Plot for Determination of Residual Capacitance.	27
17.	Plot for Determination of Residual Inductance at 5.0 Megacycles.	28
18.	Percentage Variation in Apparent Capacitance from Static C.	30
19.	Increments in Capacitance and Conductance Components Due to the Residual Inductance and Metallic Resistance.	30
20.	Current Distribution for Symmetrical Feed.	32

21.	Percentage Variation in Apparent Capacitance from Static C.	32
22.	Approximate Equivalent Circuit of Fixed Resistor.	36
23.	Mercury Cup Contact.	36
24.	A High Frequency, Variable Precision Resistor.	38
25.	Boella Behavior of Solid Carbon Resistors.	39
26.	Resistor Stray Capacitance C and Equivalent Transmission Line Circuit.	39
27.	Approximate Schematic of Resistor.	39
28.	Series Resonant Substitution Circuit.	42
29.	Coil Dissipation Factor versus Frequency.	42
30.	Series Resonant Resistance Variation Method.	46
31.	Series Resonant Reactance Variation Method.	46
32.	Resonance Curves, Reactance Variation Method.	49
33.	Parallel Resonance Substitution Method.	49
34.	Parallel Resonant Conductance Variation Method.	52
35.	Residuals, Conductance Variation Method.	52
36.	Parallel Resonance Susceptance Variation Method.	56
37.	Resonance Curves, Susceptance Variation Method.	56
38a.	Basic Conductance Substitution Circuit.	59
38b.	Equivalent Conductance Substitution Circuit.	59
39.	Simplified Indicator Circuit.	62
40.	Diode Characteristic.	62
41.	Conductance Meter Functional Diagram.	63
42.	Diode Circuit Conductance Calibration.	63
43.	Diode Circuit Voltage Coefficient.	66
44.	Residuals, Conductance Measurement Circuit.	66
45.	General Radio 916-A Radio Frequency Bridge.	68

46.	General Radio 1601 VHF Bridge.	75
47.	Effect of Inductance in Resistance Capacitor, C_A , on Indicated Resistance.	78
48.	Approximate Equivalent Circuit of C_B .	85
49.	Approximate Equivalent Circuit of C_B Including Residual Losses.	85
50.	E_A/E' versus R_e/R_L .	96
51.	Expansion of Diode Circuit Conductance Calibration.	96
52.	Expansion of Diode Circuit Conductance Calibration.	97
53.	Residuals, Reactance Variation Method.	97

CHAPTER I

INTRODUCTION

Within the last decade there has been an ever increasing demand for the development of test equipment which would be suitable for use up to 100 megacycles. The upward spiralling frequency allocations have opened an entirely new field of measurements, a difficult and barely explored field. Difficult because in the region of 100 megacycles the transitional, where lumped constant circuit and slotted line techniques overlap, is reached; we are approaching the upper limit of practical lumped constant circuits and have not quite reached the lower bounds at which distributed constant lines become important. It is here, in the span between 10 and 200 megacycles, that residual parameters become so serious a problem in impedance measuring instruments. Most instruments designed for lower frequencies are unusable because of the residuals introduced by the measuring circuits and by the external connections to the circuit to be measured. It is equally evident that at these frequencies, which are the lower limit for the use of slotted lines, the physical size of the lines becomes too great and the mechanical tolerances too close to insure reasonably accurate results. Therefore there must be developed a technique for the modification of lumped constant circuit theory to adapt it to the requirements of this frequency range.

In general there are two classes of measurement methods

that may be used at radio and very high frequencies, namely null and resonance methods. As indicated by the names, the two methods differ fundamentally only in type of indication; the first depending upon balancing to a current or voltage minimum and the latter upon tuning a resonant circuit to a current or voltage maximum. In the following tabulation, the major point of difference is in the means of obtaining the resistive component of the unknown.

I. Resonance Methods.

A. Series Resonance Methods.

- (1) Substitution
- (2) Resistance Variation
- (3) Reactance Variation

B. Parallel Resonance Methods.

- (1) Substitution
- (2) Conductance Variation
- (3) Susceptance Variation

C. Voltmeter-Ammeter Method.

- (1) Resonant Rise Method

II. Null Methods.

A. Bridge Methods.

- (1) Impedance Bridge
- (2) Modified Schering Bridge

B. Double or Twin-T Method.

1. Series resonance methods.

The series resonant methods as the name implies make use of the principles of series resonance in the secondary

circuit. It becomes obvious then that these methods would lend themselves best to the measurement of unknowns which would contribute only small series resistive values. Basically the circuit is as shown in figure 1.

The substitution method is the most straightforward of the series resonances. The secondary is first tuned to current resonance with the unknown connected in series. The unknown is then replaced by a continuously variable standard resistor set to give the same resonant deflection when C_T is retuned. It is often more satisfactory to use several fixed standard resistors which would bracket the correct current reading and then, by interpolation or plotting, arrive at an equivalent series resistance, R_i . Thus the reactance of the unknown would equal the change in reactance of the tuning capacitor and the series resistance of the unknown would equal R_i .

In the resistance variation method, the measuring circuit is resonated at the desired frequency and the scale deflection noted. Then by inserting a suitable standard resistance and noting the new reading, due to the inverse relation of meter reading to resistance, the circuit resistance can be determined. Repeating the above process with the unknown inserted in series and with the tuning capacitor reset for resonance, the difference in circuit resistances yields the unknown series resistance and the difference in tuning capacitor reactance, the unknown reactance.

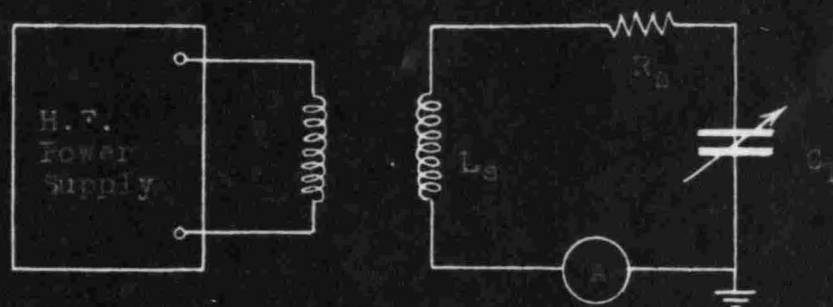
The third series resonance method, reactance variation, completely eliminates the unwieldy problem of resistance standards and makes use of the properties of the current resonance curves obtained at constant frequency by varying C_T with and without the unknown in the circuit. From the difference in the reactive values of the two settings of C_T necessary for resonance, the value of C_x is obtained. Also the unknown resistance can be deduced, as will be shown later, from the widths of the resonance curves.

There are, of course, many modifications of a practical nature that may be applied to the three series resonant methods mentioned above. These modifications are however simply refinements in techniques to arrive at more accurate results and do not basically alter the procedures outlined. It is necessary to insure that the mutual coupling be so small that variations in the secondary or measuring circuit impedance do not appreciably reflect into the primary tuned circuit. Thus the induced voltage in L_s , $-j\omega M I_p$, to all intents and purposes will be constant over the complete range of secondary variations.

2. Parallel resonance methods.

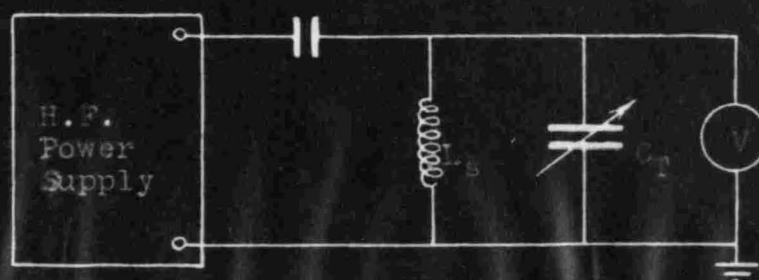
The parallel resonant methods utilize the properties of the anti-resonant L-C circuit. In general these methods are used for the measurement of high impedances. However with refinements in the indicating circuit,* low impedances can

*"An Improved Conductance Measuring Circuit," NRL Report R3133.



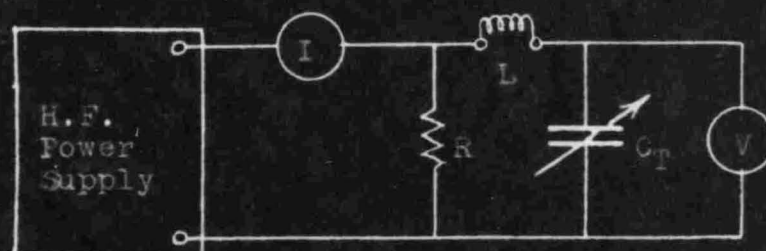
Basic Circuit, Series Resonant Method

fig. 1



Basic Circuit, Parallel Resonant Method

fig. 2



Basic Q-Meter Circuit

fig. 3

easily and accurately be determined. The basic circuit is that of figure 2.

As in the series resonant case, the substitution method is the simplest but again requires the use of a continuously variable standard resistor (in this case, high resistance) or a series of fixed high resistance standards. The circuit is first tuned to voltage resonance with the unknown connected in parallel with the L-C circuit. Then the unknown is replaced with the resistance standard and the circuit is retuned to the same resonant voltage. The unknown susceptance is given by the change in susceptance of the tuning capacitor C_T and the conductance by the reciprocal of the setting of the variable standard resistor. If a variable resistor is unobtainable, several fixed standards which will give resonant voltage readings bracketing the desired reading can be used and an interpolated value of R_p derived from the resulting plot of resonant voltage versus resistance.

The conductance variation method obviates the need for the variable standard resistor. With the unknown in parallel with L_S - C_T and C_T tuned to resonance, the resonance voltage is read with and without a parallel fixed resistor. From these readings the total conductance can be deduced. With the unknown removed and C_T retuned to resonance, the same procedure will yield the measuring circuit conductance. Thus the difference in the two circuit conductance values is the conductance of the unknown and the difference of susceptance of the settings of C_T is the susceptance of the unknown.

The susceptance variation method, the method most widely used, as in the series resonance case, makes use of the width of the resonance curve of voltage versus tuning capacitor setting. One such curve is taken with the unknown connected in parallel. Then, removing the unknown, the resonance curve of the measuring circuit is plotted. From the breadth of the two curves, the two conditions of conductance can be deduced. Thus the unknown conductance is the difference; the unknown susceptance, the difference in susceptance of the tuning capacitor setting at the peaks of the resonance curves.

In each of these parallel resonance methods, the capacitive coupling C_c is made so small that tuning the measuring circuit has no appreciable effect on the frequency or amplitude of the high frequency current source.

3. Voltmeter-ammeter method.

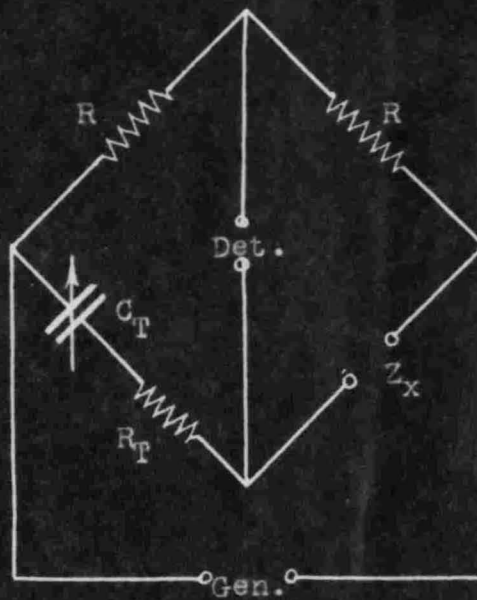
One of the more popular of the resonant rise of voltage methods is the so-called Q-meter. In essence it is a single series resonant circuit as shown in figure 3.

The resistance R is made so small that any variation in the measuring circuit has no appreciable effect on the IR drop across it; i.e. I is essentially constant. There are two methods of inserting the unknown to be measured, either in series with the resonating coil L_s or in parallel with C_T . In general small impedances are best measured by series injection and large impedances by parallel injection. In any case, when the measuring circuit is resonated at the

desired frequency, the ratio of the resonant rise of voltage V across the capacitor C_T to the constant input voltage E is the measure of this effective Q of the circuit. The voltmeter can be calibrated to read Q_e directly. By resonating the measuring circuit with and without the unknown connected and noting the values of Q_e and C_T in each case, the effective series or parallel parameters of the unknown can be deduced. There are many precautions necessary for precise, high frequency measurements with this instrument; these will be enumerated with further development of the circuit.

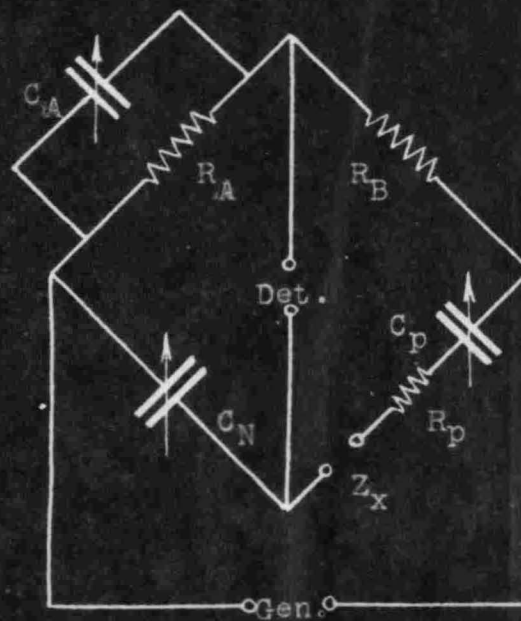
4. Bridge methods.

One of the simplest bridge circuits used today for impedance measurements at radio frequencies is the equal arm impedance bridge, the greatly simplified circuit of which is shown in figure 4. It is obvious that balance exists when the two lower arms are of equal impedance. There are several methods of utilizing the circuit; one, by inserting the unknown in the lower right arm and two, by placing a suitable impedance in the lower right arm and balancing the bridge with and without the unknown in series with the standard arm. In the first case, the settings of the tuning capacitor and the standard variable resistor give the constants of the unknown directly. In the second case, the difference in reactance of the capacitor settings is the unknown reactance and the difference in standard resistor settings, the unknown resistance.



Impedance Bridge-Basic Circuit

fig. 4



Modified Schering Bridge-Basic Circuit

fig. 5

A more widely used bridge is the modified Schering bridge shown schematically in figure 5. It eliminates the need for the unsatisfactory variable resistance standard of the impedance bridge by making the balance dependent upon the settings of the variable air capacitors, C_A and C_P . In making measurements, the bridge is first balanced with a short circuit placed across the unknown terminals. Then, replacing the short circuit with the unknown and rebalancing, it can be shown that

$$R_x = \frac{R_B}{C_N} (C_{A2} - C_{A1}) \quad (1)$$

$$X_k = \frac{1}{\omega} \left(\frac{1}{C_{P2}} - \frac{1}{C_{P1}} \right) \quad (2)$$

where C_{A1} , C_{P1} and C_{A2} , C_{P2} are respectively the initial and final capacitor settings. Features of the bridge are such that the tuning capacitor C_A can be calibrated to read resistance in ohms directly and that C_P can be calibrated to read reactance directly in ohms at any one given frequency, say 10 or 100 megacycles.

5. The Twin-T circuit.

The Twin-T circuit, while not a bridge circuit in the accepted sense of the word, naturally falls under the classification of null methods. It is a comparatively new idea and has certain inherent advantages over the accepted bridge circuits. Because one terminal of each of C_B (the susceptance capacitor), C_G (the conductance capacitor), L , the generator and the detector is tied directly to

ground, the need of a transformer is eliminated. Also certain residual stray capacitances are excluded from the calculations of the unknown parameters. Capacitances from points "a" and "c" to ground fall across the generator and the detector and therefore do not enter into the balance conditions. Similarly, stray capacitances from points "b" and "d" to ground are in parallel with C_B and C_G in both the initial and final balance positions and thus have no effect on the measurement of the unknown since only the change of capacitance settings is of importance. Stray capacitances across C' , C'' , and C''' affect balance conditions but introduce no error if they are included in the original calibration. The residual capacitance across R will of course affect its characteristics. However this can be beneficial if of the right order of magnitude by balancing out to some extent the residual inductance of the standard resistor.

Direct capacitances may exist between points "a"- "c" and "b"- "d" and they must be minimized by shielding.

Thus the Twin-T provides a method of measuring the unknown conductance and susceptance by direct substitution methods and of making the results direct reading on calibrated, precision, variable air capacitor dials. The balance conditions are given by

$$G_L - R\omega^2 C' C'' \left(1 + \frac{C_G}{C'''}\right) = 0$$

and
$$C_B + C' + C''' + \frac{C'C''}{C'''} - \frac{1}{\omega^2 L} = 0$$

The unknown parameters, assuming that there are no residuals existent, follow:

$$G_x = R\omega^2 C' C'' (C_{G2} - C_{G1}) / C''' \quad (3)$$

$$B_x = \omega (C_{B1} - C_{B2}) \quad (4)$$

where the subscripts indicate the initial and final readings.

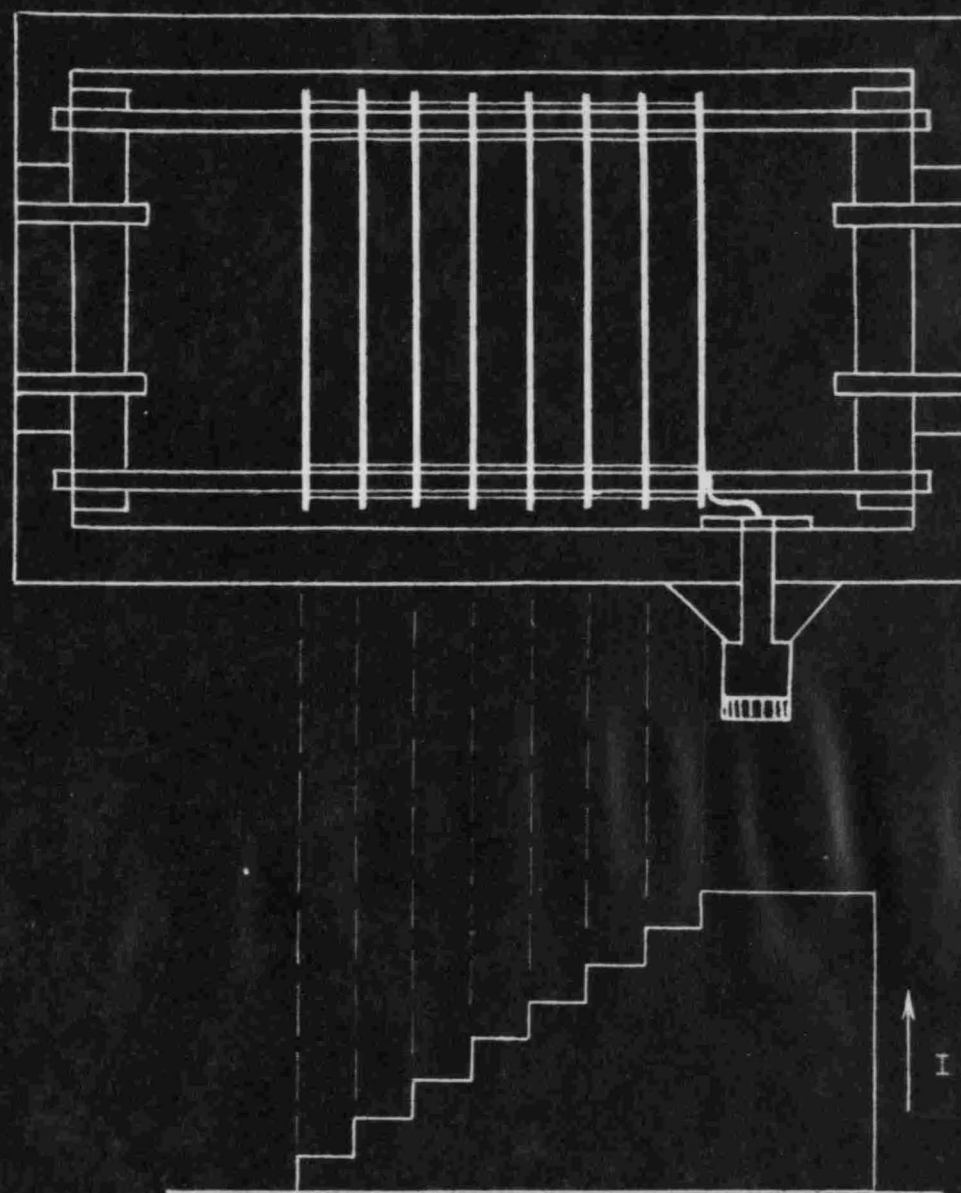


CHAPTER II

THE CAPACITANCE STANDARD

One of the most important tools is the precision standard, variable air capacitor. Even the most casual inspection of the introduction to high frequency measuring techniques reveals that indeed this capacitor is the backbone of all measurements. However, the assumption that it is a purely reactive, dissipationless element is untenable at these high frequencies and a closer examination of the nature of this standard is in order to determine as precisely as possible its residual parameters. It is these residuals that primarily fix the upper frequency limits at which measurements may be made.

It would be well at this point to examine the structure of a typical precision capacitor (General Radio Type 722-M) and endeavor to isolate the sources of residuals. Figure 7 is a rough approximation of the stator and its supporting frame. The current flows in through the terminal post to the top stator plate. Here the current follows two paths; a small portion passes out through the stator plate to the rotor plate and back to the ground post. The remaining current flows down the stator lead to the second stator plate where a similar division occurs. This process continues along the stack to the last plate. This current distribution sets up, in the plane of the plates, a magnetic flux. The currents in the plates themselves have very little



Stator Structure of Typical Precision Capacitor.
Current Distribution in Stator Stack Supports.

fig. 7

affect on this flux density since they are diffused over relatively large areas and are shielded to some extent by the plates. There is then a residual inductance associated with this flux distribution and such inductance must be confined primarily to the stator leads and stator supports. Also, the inductance must remain relatively constant irrespective of capacitor setting. This assumption leads to the following representation of a dissipationless capacitor. See figure 8. This type of circuit has multiple resonances depending upon the number of sections but at operating frequencies low enough to insure that the effective capacitance is within a few percent of the static value, it can be further simplified. See figure 9. The effective input capacitance can be found from

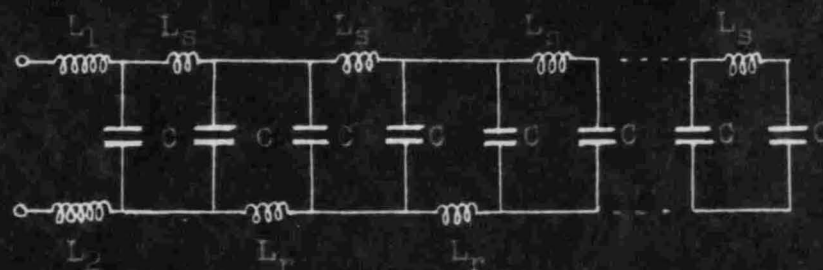
$$-j\frac{1}{\omega C_e} = j(\omega L - \frac{1}{\omega C})$$

or

$$C_e = \frac{C}{1 - \omega^2 L C} \quad (5)$$

Thus it is evident that the residual inductance makes the effective input capacitance larger than the static value, C.

In addition to the residual inductance, there are certain losses which must now be considered, losses in both the metal and dielectric structures. The dielectric losses will occur in the isolantite or fused quartz supports at the top and bottom of the stator stack. These supports lie in a field which is independent of rotor position but dependent upon voltage. Therefore at any one frequency,



C = Static capacitance between any stator plate and one adjacent rotor plate.

L_1 = Inductance of stator lead.

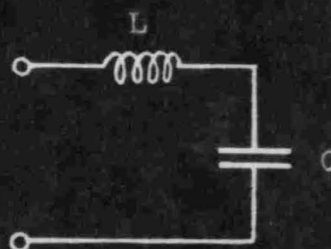
L_2 = Inductance of rotor lead.

L_s = Inductance of section of stator support between any two adjacent stator plates.

L_r = Inductance of section of rotor support between any two adjacent rotor plates.

Equivalent Circuit of Dissipationless Precision Capacitor

Fig. 8



L = Total residual inductance.

C = Total residual capacitance.

Simplified Equivalent Circuit

Fig. 9

it can be assumed that these losses are constant and can be represented by two conductances, G_{top} and G_{bot} . The metallic losses will occur in all metal parts but will be localized almost entirely in contact resistances in the bolted assemblies and in the sliding rotor contacts. Again it can be said that these losses will be essentially independent of rotor position. Expanding the equivalent circuit then yields figure 10.

With the previous assumptions this can be simplified to the circuit of figure 11.

Deriving the input impedance from this simplified circuit,

$$\begin{aligned} Z_{IN} &= (R + j\omega L) - \frac{j \frac{1}{\omega C G}}{\frac{1}{G} - j \frac{1}{\omega C}} \\ &= R + \frac{G}{G^2 + \omega^2 C^2} - j \left[\frac{C}{G^2 + \omega^2 C^2} - \omega L \right] \end{aligned}$$

If $G^2 \ll \omega^2 C^2$

$$Z_{IN} = R_e - j \frac{1}{\omega C_e} = \left(R + \frac{G}{\omega^2 C^2} \right) - j \left(\frac{1 - \omega^2 L C}{\omega C} \right)$$

where $R_e = R + \frac{G}{\omega^2 C^2}$ (6)

and $C_e = \frac{C}{1 - \omega^2 L C}$ (5)

Similarly

$$Y_{IN} = \frac{R\omega^2 C^2 + G}{(1 - \omega^2 L C)^2 + \frac{(R\omega^2 C^2 + G)^2}{\omega^2 C^2}} + j \frac{\frac{\omega C}{1 - \omega^2 L C}}{(1 - \omega^2 L C)^2 + \frac{(R\omega^2 C^2 + G)^2}{\omega^2 C^2}}$$

At 10 to 100 megacycles, the denominator is very nearly equal to unity. Thus

$$Y_{in} = [R(\omega C)^2 + G] + j \left[\frac{\omega C}{1 - \omega^2 LC} \right]$$

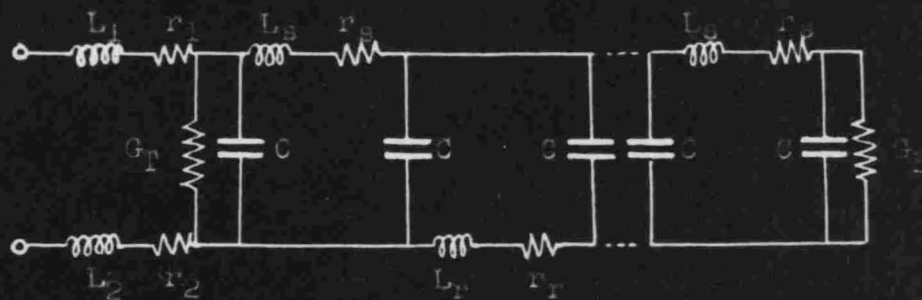
and $G_e = R(\omega C)^2 + G \quad (7)$

Examination of these equations reveals that the dielectric losses introduce a resistive component which is a function of both frequency and rotor setting and the metallic losses introduce a conductive component equally a function of frequency and setting. The residual inductance increases the effective input capacitance which is dependent upon frequency and rotor setting. However the effects of residuals upon the absolute values of capacitance are not as interesting as the effects on the capacitive differences. For it is these differences that are used primarily to determine the unknown impedance. Thus

$$\begin{aligned} \Delta C_e &= C_{e1} - C_{e2} = \frac{C_1}{1 - \omega^2 LC_1} - \frac{C_2}{1 - \omega^2 LC_2} \\ &= \frac{C_1 - \omega^2 LC_1 C_2 - C_2 + \omega^2 LC_1 C_2}{(1 - \omega^2 LC_1)(1 - \omega^2 LC_2)} \\ &\doteq \frac{C_1 - C_2}{1 - \omega^2 L(C_1 + C_2) + \omega^4 L^2 C_1 C_2} \end{aligned}$$

At 100 megacycles

$$\Delta C_e \doteq \frac{C_1 - C_2}{1 - \omega^2 L(C_1 + C_2)} \quad (8)$$



$L_1, L_2, L_S, L_F, C =$ (See figure 8)

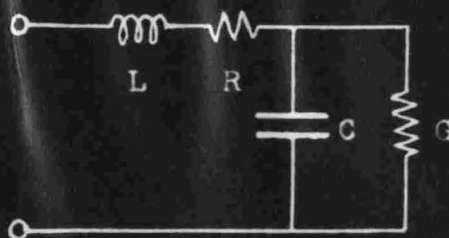
$G_T =$ Equivalent conductance of top dielectric supports.

$G_B =$ Equivalent conductance of bottom dielectric supports.

$r_1, r_2, r_s, r_r =$ Series contact resistance in bolted structures and rotor contacts.

Equivalent Circuit of Precision Capacitor

fig. 10



$L =$ Total residual inductance.

$C =$ Total static capacitance.

$R =$ Total ohmic and eddy current residual resistance.

$G =$ Total dielectric residual conductance.

Simplified Equivalent Circuit of Precision Capacitor

fig. 11

Also

$$\Delta G_e = G_{e1} - G_{e2} \doteq R[(\omega C_1)^2 - (\omega C_2)^2]$$

$$= R\omega^2 [(C_1 - C_2)(C_1 + C_2)] \quad (9)$$

Correspondingly,

$$\Delta S_e = S_{e1} - S_{e2} = (S_1 - S_2) \quad (10)$$

and

$$\Delta R_e = R_{e1} - R_{e2} \doteq \frac{G}{\omega^2} \left(\frac{1}{C_1^2} - \frac{1}{C_2^2} \right)$$

$$= \frac{G}{\omega^2} \left[\frac{(C_2 + C_1)(C_2 - C_1)}{C_1^2 C_2^2} \right] \quad (11)$$

It can be seen from the equations above that the dielectric losses $(G/\omega^2 C^2)$ are predominant at low frequency while the metallic losses $(R\omega^2 C^2)$ are of importance at high frequency. The error caused by residual inductance in the capacitance increment is not equal to the average error at the two settings but is rather more nearly equal to the sum of the errors. The change in conductance or rather in the metallic losses component is directly proportional to the square of the capacitance. The elastance component however, since the residual inductance is a constant series element, is errorless in taking elastance differences. The dielectric losses component of the resistive measurement introduces an error which is directly proportional to the square of the elastances or inversely proportional to the square of the capacitances.

Thus, in the parallel substitution method, the residuals of the tuning capacitor will introduce errors in

both the conductance and susceptance measurements. In the series substitution method, errors appear in the resistive measurement, but not in the reactive.

If the immediate exterior circuit is examined for errors closely allied with the tuning capacitor, a small stray capacitance, in the series substitution method, will be introduced by the insertion of the unknown in the measuring circuit. This C_s appears directly across the terminals of the standard as shown in figure 12. The impedance looking into the standard is

$$Z_{in} = \frac{(R_e - j\frac{1}{\omega C_e})(-j\frac{1}{\omega C_s})}{R_e - j(\frac{1}{\omega C_e} + \frac{1}{\omega C_s})}$$

which reduces to

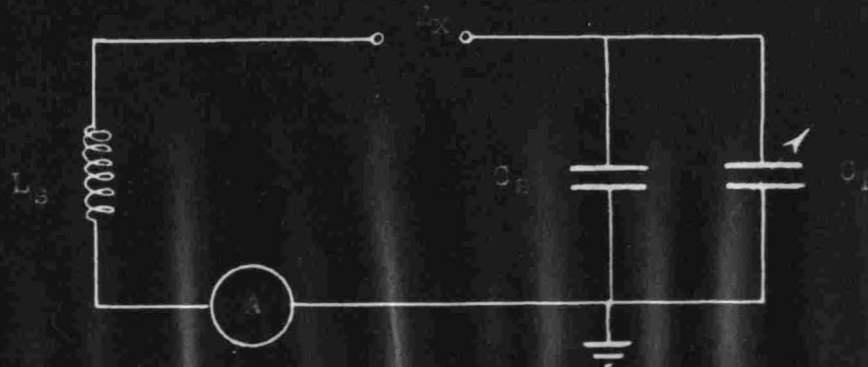
$$\begin{aligned} Z_{in} &= \frac{\frac{R_e}{(\omega C_s)^2} - j \left[\frac{R_e^2}{\omega C_s} + \frac{C_e + C_s}{\omega (\omega C_e C_s)^2} \right]}{R_e^2 + \left(\frac{C_e + C_s}{\omega C_e C_s} \right)^2} \\ &= \frac{R_e C_s^2}{(\omega C_e C_s R)^2 + (C_e + C_s)^2} - \frac{j (\omega C_e R)^2 C_s + (C_e + C_s)}{\omega (\omega C_e C_s R)^2 + (C_e + C_s)^2} \end{aligned}$$

At 100 megacycles, where $C_s = 10^{-11}f$,

$$Z_{in} \doteq R_e - j \frac{1}{\omega (C_e + C_s)} \quad (12)$$

Therefore

$$\begin{aligned} \Delta S_e &= \frac{S_{e1}}{1 + C_s S_{e1}} - \frac{S_{e2}}{1 + C_s S_{e2}} \\ &\doteq \frac{S_1 - S_2}{1 + C_s (S_1 + S_2)} \quad (13) \end{aligned}$$



Parallel Stray Capacitance

fig. 12

Thus the reactive measurement is no longer independent of residuals associated with the tuning capacitor but is clearly dependent upon the stray capacitance introduced across the terminals of the standard.

From equations (8), (9), (11) and (13) can be seen the nature of the dependency of the errors upon the residual parameters associated with the standard tuning capacitor. In each instance, the errors are dependent upon the rotor setting. If an unknown fixed capacitor were then to be measured by a substitution method, its impedance and admittance would vary with initial setting of the tuning capacitor.

Thus, solving for C_x and G_x by parallel substitution and S_x and R_x by series substitution, by rewriting equations (8), (9), (11) and (13),

$$C_x = \frac{C_1 - C_2}{1 - \omega^2 L (C_1 + C_2)} \quad (8a)$$

$$G_x = R\omega^2 (C_1 - C_2)(C_1 + C_2) - \Delta G_o \quad (9a)$$

$$R_x = \frac{G}{\omega^2} (S_1 - S_2)(S_1 + S_2) - \Delta R_o \quad (11a)$$

and
$$S_x = \frac{S_1 - S_2}{1 + C_s (S_1 + S_2)} \quad (13a)$$

where G_o and R_o are the changes in circuit conductance and resistance with the unknown in and out of the circuit. But

$$(C_1 - C_2) \doteq C_x$$

and
$$(S_1 - S_2) \doteq S_x$$

$$G_x = R\omega^2 C_x (C_1 + C_2) - \Delta G_o \quad (9b)$$

$$R_x = \frac{G}{\omega^2} S_x (S_1 + S_2) - \Delta R_o \quad (11b)$$

From (8a) a plot of $(C_1 - C_2)$ versus $(C_1 + C_2)$ yields a straight line of slope $-LC_x$ and ordinate intercept of C_x . Equation (9b), plotted with G_o versus $(C_1 + C_2)$, is a straight line with a slope of $R\omega^2 C_x$ and intercept of $-G_x$. A plot of (11b) with R_o versus $(S_1 + S_2)$ yields a straight line of slope GS_x/ω^2 and intercept $-R_x$. Similarly, (13a), with $(S_1 - S_2)$ versus $(S_1 + S_2)$ yields a straight line of slope $C_S G_x$ and intercept S_x .

Thus, by measuring a large range of unknown fixed capacitors and plotting the results as above, a very good means of determining L , R , G and C_g of the variable standard capacitor is available. Typical plots (see figures 13, 14, 15 and 16) of experimental data taken by resonance methods at 1.5 megacycles on a General Radio type 222-M precision capacitor yield the following residual parameters:

$$L = 0.0604 \mu h$$

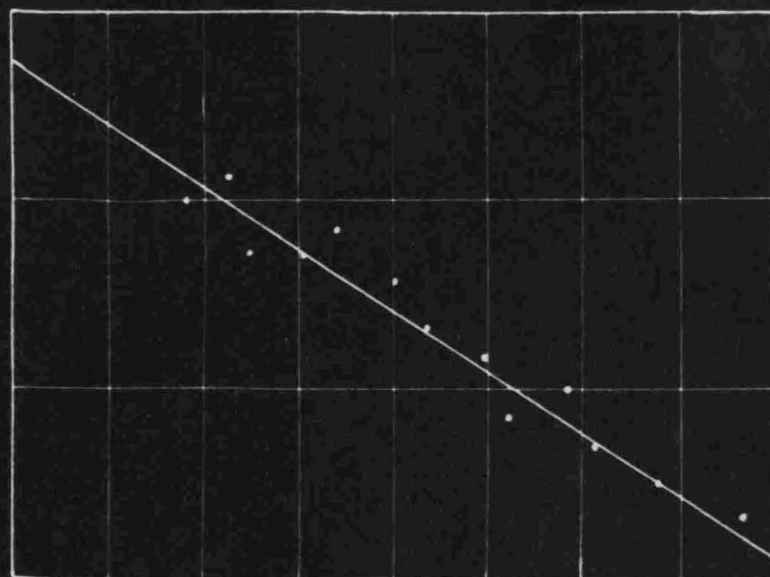
$$R = 0.017 \text{ ohms}$$

$$C_S = 2.4 \mu\mu f$$

$$G = 0.210 \text{ micromhds}$$

Further experimental results at 5.0 megacycles for the determination of L (see figure 17) show the increase of accuracy with increasing frequency. This method of attack, using parallel and series substitution methods, should prove useful and accurate up to a frequency of 30 megacycles.

$(C_1 - C_2)$ in $\mu\mu f$

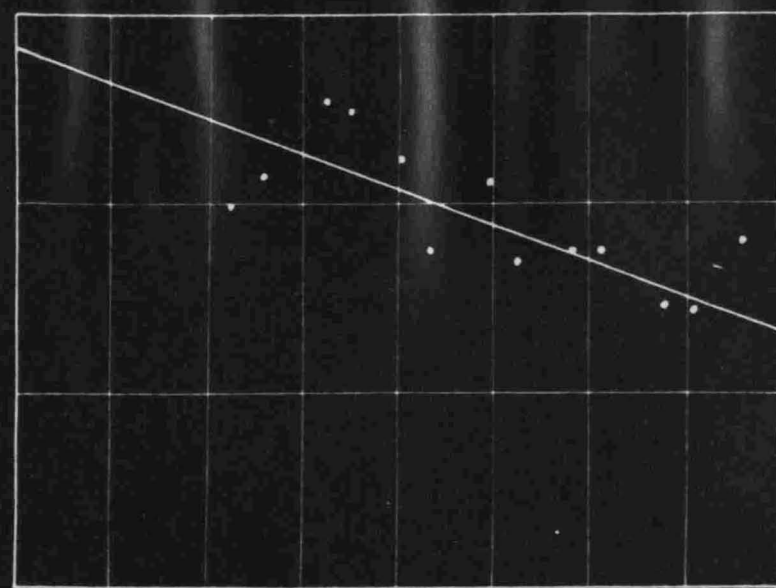


$(C_1 + C_2)$ in $\mu\mu f$

Plot for Determination of Mutual Inductance of Parallel Wires

Fig. 13

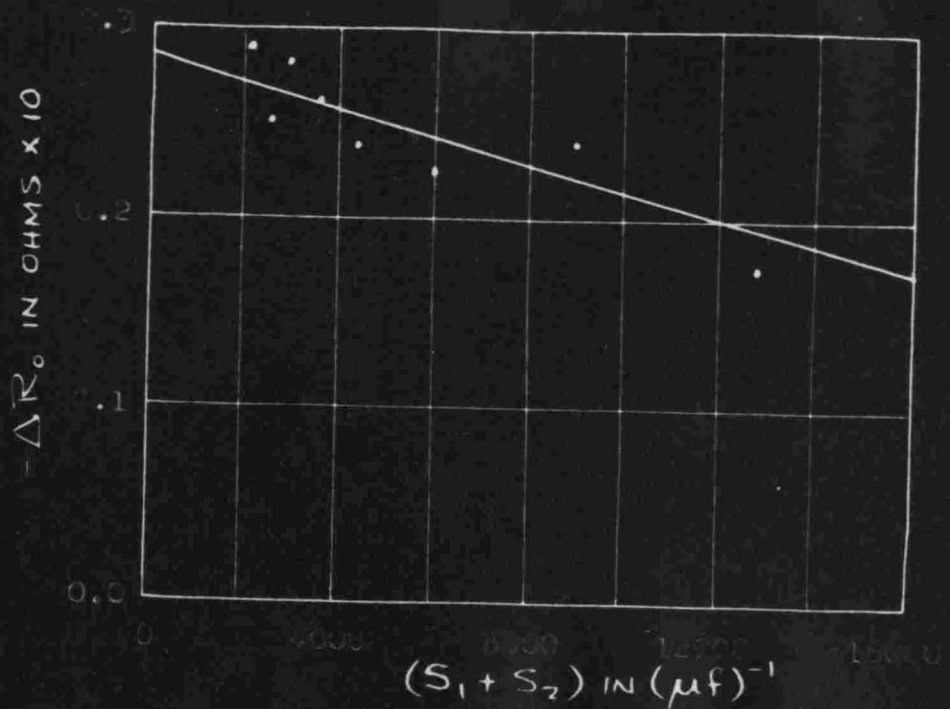
$-\Delta G_0$ in $\mu mhos$



$(C_1 + C_2)$ in $\mu\mu f$

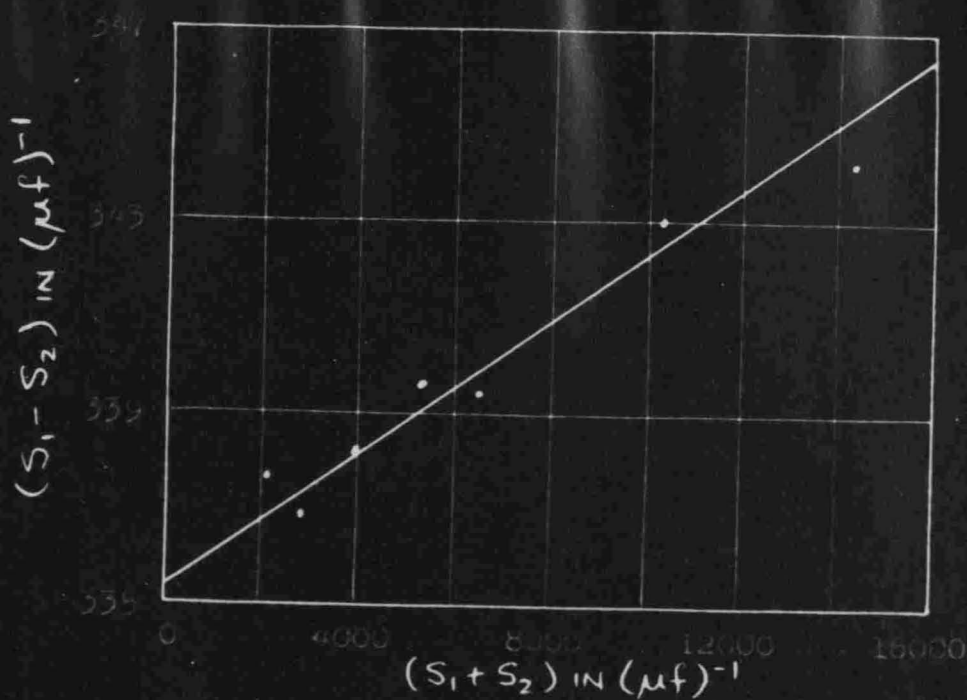
Plot for Determination of Mutual Resistance

Fig. 14



Plot for Determination of Residual Capacitance

Fig. 15



Plot for Determination of Residual Capacitance

Fig. 16

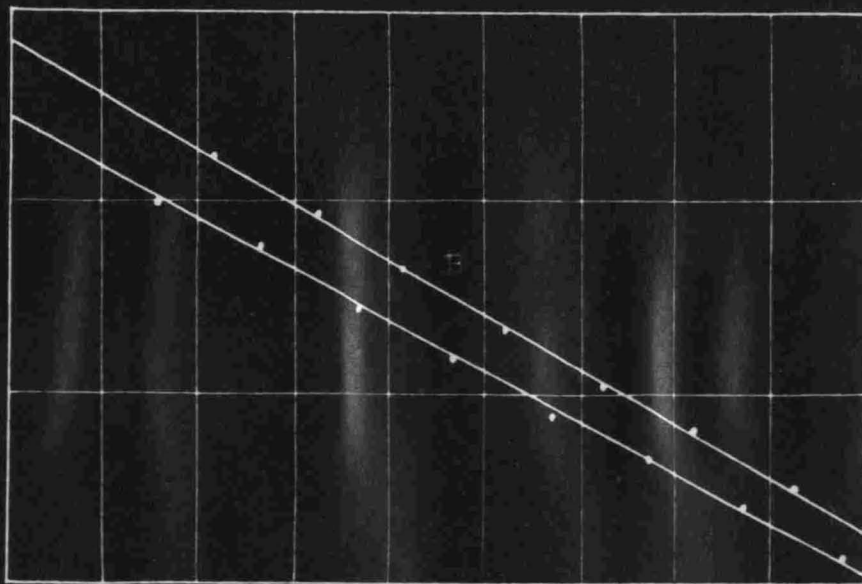
$(C_1 - C_2)$ in μmf

198 94

190 90

182 86

174 82



$(C_1 + C_2)$ in μmf

Plot of Deposition Rate vs. Time

Deposition Rate

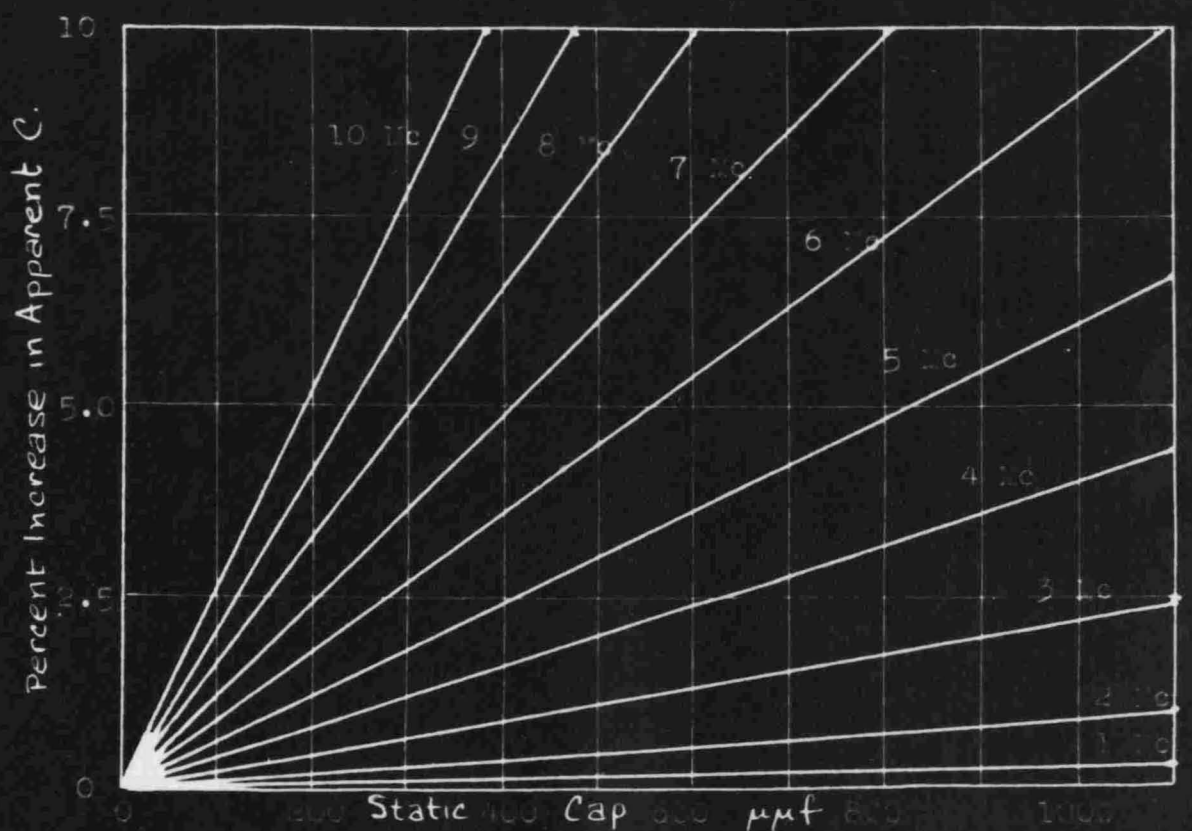
Time

Above this limit, external residual parameters in the series substitution method (to be discussed below) become exceedingly difficult to cope with. However, the experimental data could be obtained, using a modified Schering bridge, at frequencies in the neighborhood of 100 megacycles.

In figure 18 the percentage variation in apparent capacitance from the static value is plotted versus static capacitance for frequencies from 1 megacycle to 30 megacycles. The residual inductance of only $0.0591 \mu h$ obviously makes the bland acceptance of capacitance readings without necessary corrections out of the question. At a maximum setting of $1100 \mu f$, the apparent capacitance has increased by more than a quarter percent at 1 megacycle and by 10 percent at 6 megacycles.

A study of input capacitance shows that at low frequencies, where dielectric losses predominate, the conductance is constant at any one frequency independent of rotor setting. However at higher frequencies, where the metallic losses become so important and are directly proportional at any one frequency to the square of the capacitance setting, the input conductance is no longer constant and such an assumption is seriously in error. The plots in figure 19 make this fact evident.

Certain design features will reduce several of the residuals appreciably. The current distribution along the stator and rotor shafts is essentially as shown in figure 7. To a first approximation this can be assumed to be a linear



Percentage Variation in Apparent Capacitance from Static C

fig. 18

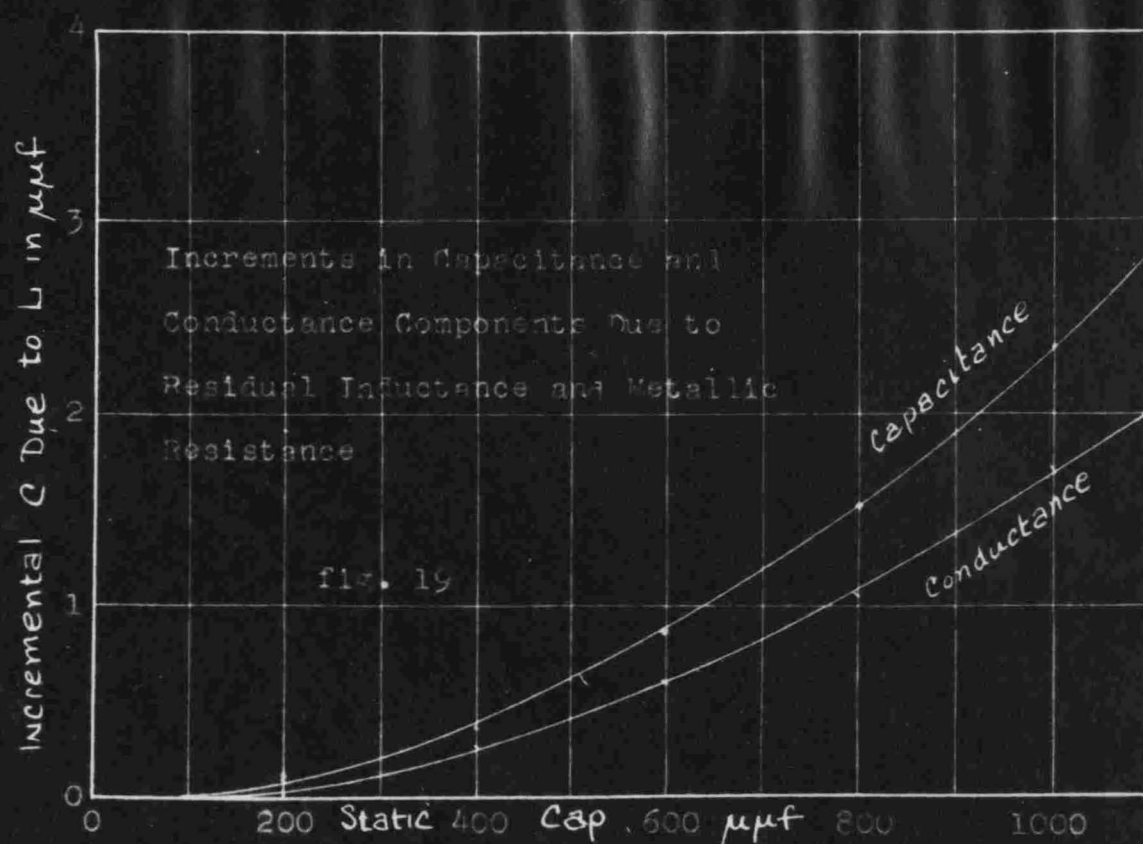


fig. 19

distribution. If R is the resistance and L the inductance of the rotor shaft to uniform current distribution, the effective residuals from non-uniform linear current can be determined from energy relations to be

$$R_e = \frac{R}{3} \qquad L_e = \frac{L}{3} \qquad (14)$$

These values can be reduced by symmetrical feed systems shown diagrammatically in figure 20 where (a) is center feed, (b) dual feed, and (c) triple feed. For center feed, energy relations yield

$$R_e = \frac{R}{12} \qquad L_e = \frac{L}{12}$$

Further multiple feed reduces the effective resistance and inductance by

$$R_e = \frac{R}{12n^2} \qquad L_e = \frac{L}{12n^2} \qquad (15)$$

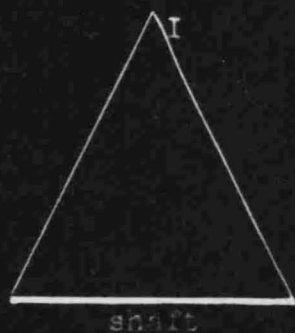
where "n" is the number of feed points. These features have been incorporated in the General Radio type 722-N precision capacitor, particularly designed for high frequency work with center feed to the rotor shaft. At 1.5 megacycles it has the following residual parameters:

$$L = 0.024 \mu h$$

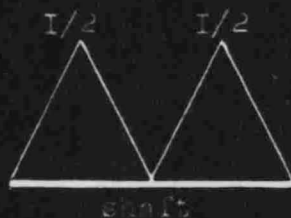
$$R = 0.008 \text{ ohms}$$

$$G = 0.3 \mu mhos.$$

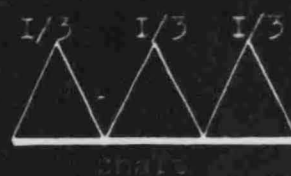
Thus the residual inductance has been reduced by 60 percent, the residual metallic resistance by over 50 percent. Based



(a)



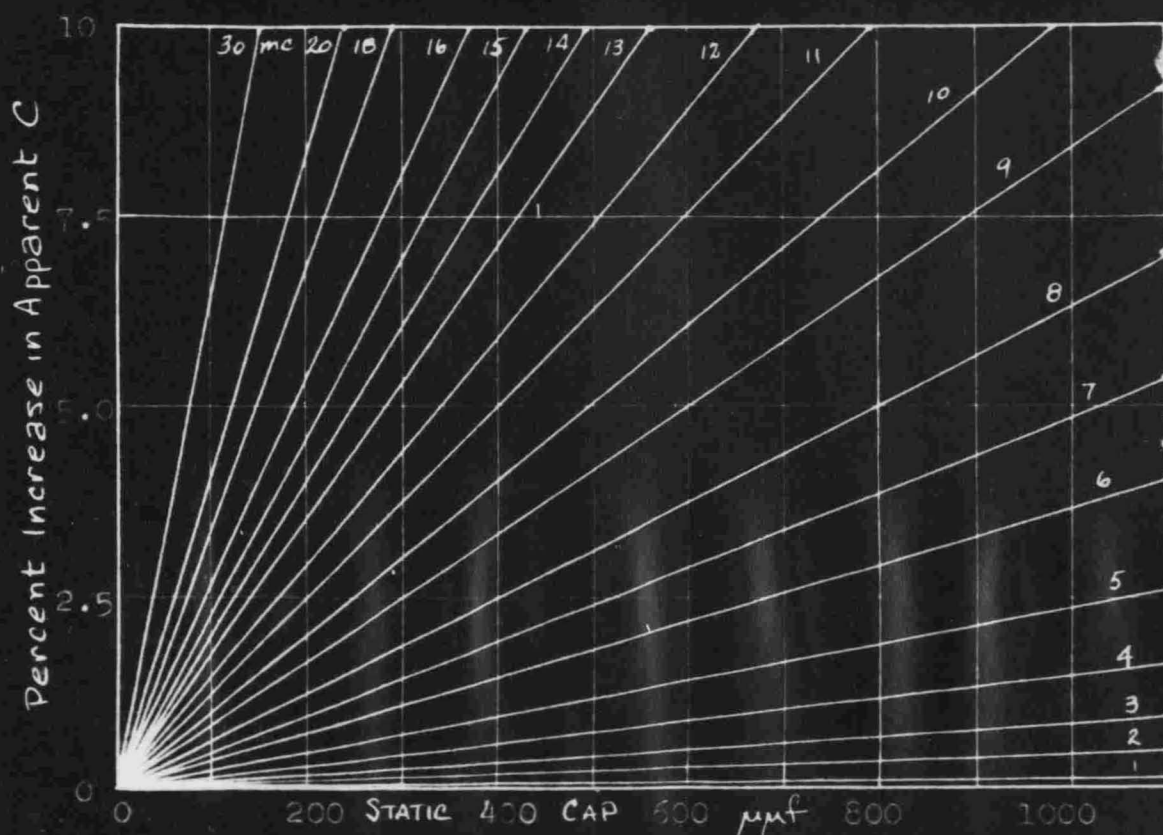
(b)



(c)

Current Distribution for Symmetrical Test

fig. 20



Percentage Variation in Apparent Capacitance from Static C

fig. 21

on these figures, figure 21 indicates a decreased percentage rise of effective capacitance versus static capacitance at any one frequency. For instance, from figure 18, at 6 megacycles and a setting of 1100 $\mu\mu\text{f}$, there is a 10 percent rise in effective capacitance. From figure 21, the 722-N capacitor shows less than 4 percent rise at 6 megacycles and 1100 $\mu\mu\text{f}$ setting. Further experimental information seems to indicate that there are practical limits to the number of feedpoints that can satisfactorily be employed. Also it is extremely difficult to realize a residual inductance L less than 0.006 μh and R less than 0.002 ohms.

CHAPTER III

THE RESISTANCE STANDARD

One of the most difficult problems encountered in the field of high frequency measurements today is the design of a continuously variable, standard resistor such as that required in the substitution method of both the series and parallel resonant circuits. Equally as difficult is the use of fixed, high frequency, standard resistors as required by the resistance variation and conductance variation methods. It is exactly these problems which contribute to the limiting of the present useful frequency range of the above mentioned measuring circuits.

Figure 22 is an approximate equivalent circuit of a fixed resistor. L represents the series inductance of the resistor and C , the parallel stray capacitance. The input impedance is given by

$$\begin{aligned} Z_{in} &= \frac{(R + j\omega L)(-j\frac{1}{\omega C})}{R + j(\frac{\omega^2 LC - 1}{\omega C})} \\ &= \frac{R - j[\omega L(\omega^2 LC - 1) + \omega CR^2]}{(\omega CR)^2 + (\omega^2 LC - 1)^2} \quad (16) \end{aligned}$$

$$R_e = R / [(\omega CR)^2 + (\omega^2 LC - 1)^2] \quad (17)$$

$$G_e = R / (\omega^2 L^2 + R^2) \quad (17a)$$

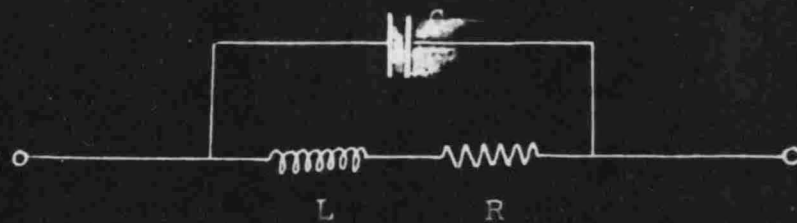
$$X_e = -j \left[\frac{\omega L(\omega^2 LC - 1) + \omega CR^2}{(\omega CR)^2 + (\omega^2 LC - 1)^2} \right] \quad (18)$$

$$B_e = j\omega [L(\omega^2 LC - 1) + CR^2] \quad (18a)$$

If R is large, $(\omega CR)^2$ is large and R_e decreases with frequency. With a small R , $(\omega CR)^2$ is small and, as $\omega^2 LC$ approaches unity, $(\omega CR)^2 + (\omega^2 LC - 1)^2 \ll 1$ and R_e increases rapidly.

At 100 megacycles the contact resistance introduced when the fixed resistor is inserted in, say, the resistance variation circuit must also be considered. Even with mercury cups, this resistance component cannot be made negligibly small nor can it be made constant. This non-uniformity can be a large percentage of the inserted resistance. Also at these frequencies, the possibility of contact resistance skin effect must be examined. Consider the following diagram, figure 23. There is the distinct possibility, in fact, an almost certainty that there will not be perfect contact throughout the area of contact, that contact may exist only near the center of the conductor. And at 100 megacycles, the center of the conductor carries essentially no current. Thus the skin currents in the conductor must flow through an added resistance in the contact and this resistance can well be attributed to contact skin effect.

The continuously variable, standard resistor has been solved in one aspect by Weaver and McCool in their work at the Naval Research Laboratories. In the design of their variable diode conductance measuring circuit (to be discussed below), they have adapted the characteristics of the diode to provide a parallel circuit, variable conductance, stable and suitable to accurate calibration at 10 megacycles.



Approximate Equivalent Circuit of
Fixed Resistor

fig. 22

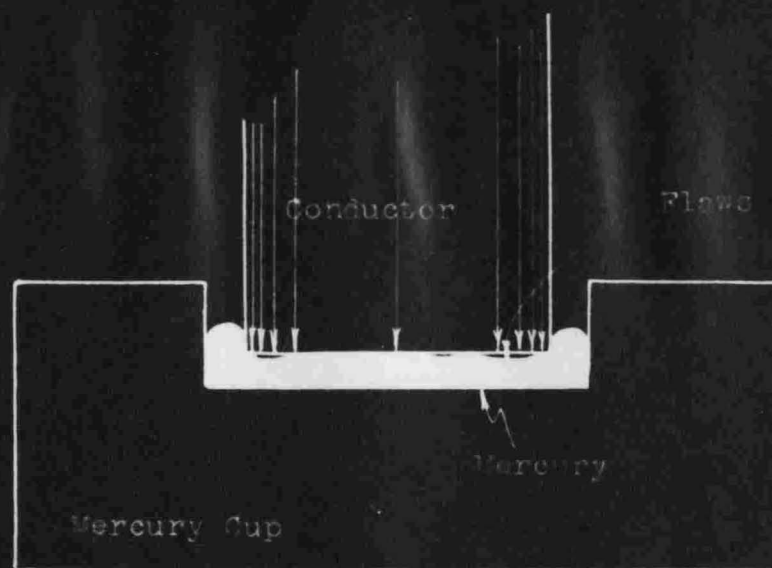
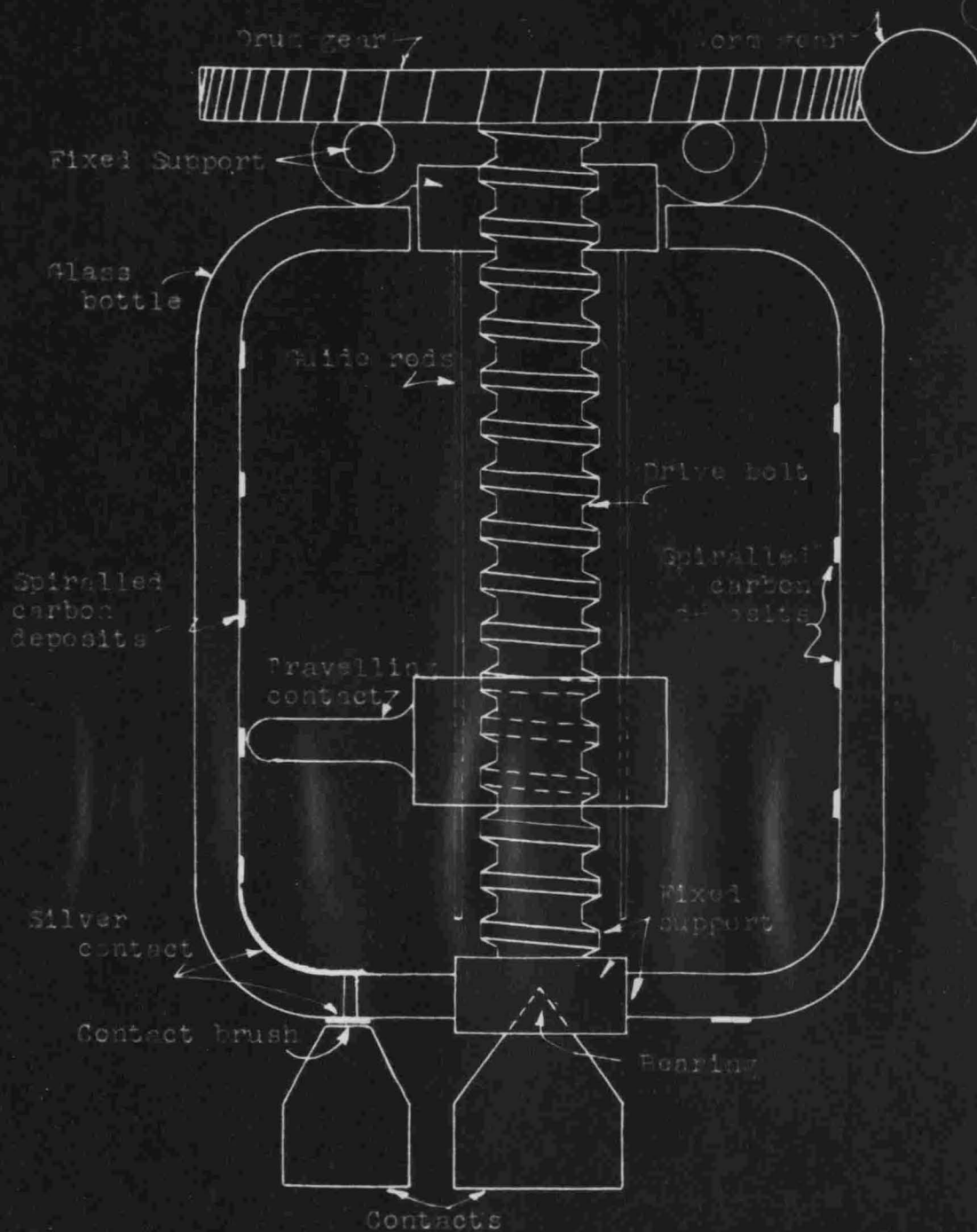


fig. 23

However there are no continuously variable, mechanical resistors suitably precise at these frequencies. There are new processes available though for the use of carbon deposits in the manufacture of high frequency, large valued resistances. It is thought possible that, using these processes, some sort of mechanical structure such as that of figure 24 might be feasible. It is a nice problem that will bear a great deal of thought and experimentation.

The greatest difficulty to overcome in the design of a high frequency, high valued resistor is the Boella effect, so called after one of the men instrumental in its discovery in the early 1930's. It has been shown and experimentally verified that all resistors above a given nominal value drop off sharply in a.c. resistance with increasing frequencies. Boella, G. W. O. Howe and several others have shown that the following plot, figure 25, of R_{ac}/R_{dc} versus kfR_{dc} (where f is in cycles and R_{dc} is in ohms) is representative.

This resultant drop in the ratio R_{ac}/R_{dc} is attributed to the characteristics of the parallel shunt of the residual stray capacitance. There is an electrostatic field built from the resistor causing a definite incremental, stray capacitance to be associated with each segment of length. Thus as in figure 26, the resistor can be thought of as a symmetrical transmission line. G. W. O. Howe also has plotted the input capacitance and arrived at a result similar in shape to figure 25.



A High Frequency, Variable Precision Resistor

fig. 24

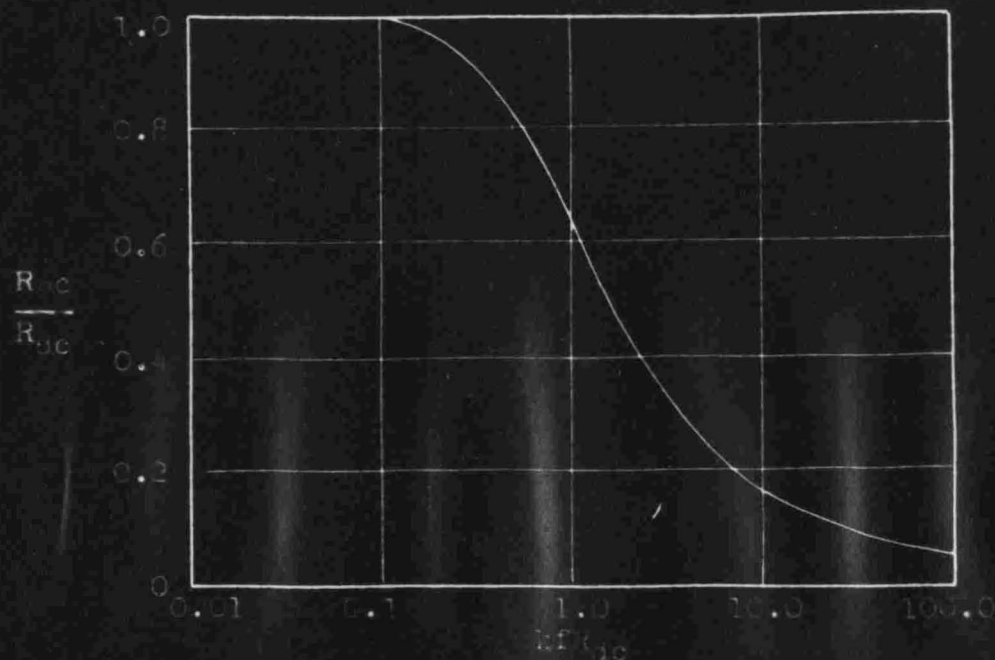
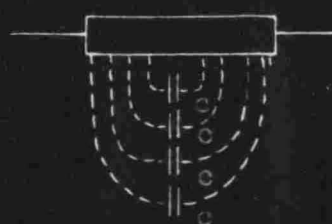
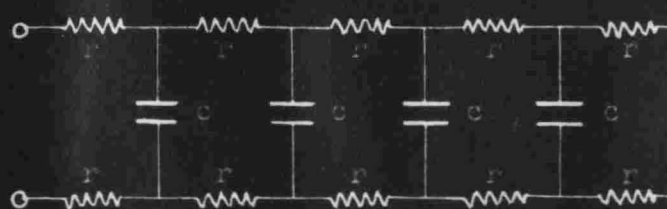


Fig. 25. Resistor Behavior of Soil Carbon Resistors

Fig. 26

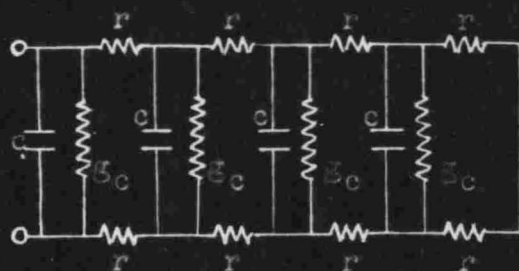


Resistor Array
Capacitance c

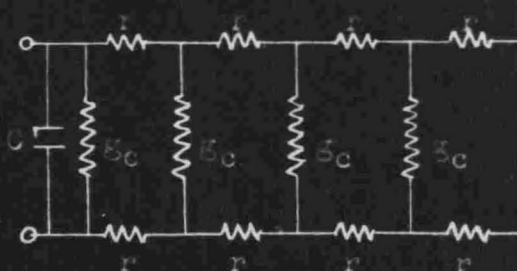


Equivalent Transmission Line
Circuit

Fig. 26



\approx



Approximate Schematic of Resistor

Fig. 27

Further experimentation by R. F. Field of General Radio Company on many different types of high valued resistors has further verified the Boella effect. However his measurements have shown that the shunt capacitance as plotted against fR_{dc} (where f is in megacycles and R_{dc} is in megohms) is essentially constant; there is no apparent Boella contour. To explain the decrease in R_{ac} , Mr. Field proposes that the stray capacitors be resolved into their effective shunt capacitance and shunt conductance. This would lead to a schematic as shown in figure 27. Thus the dielectric losses in the stray capacitance account for the R_{ac} variation.

CHAPTER IV

SERIES RESONANCE METHODS

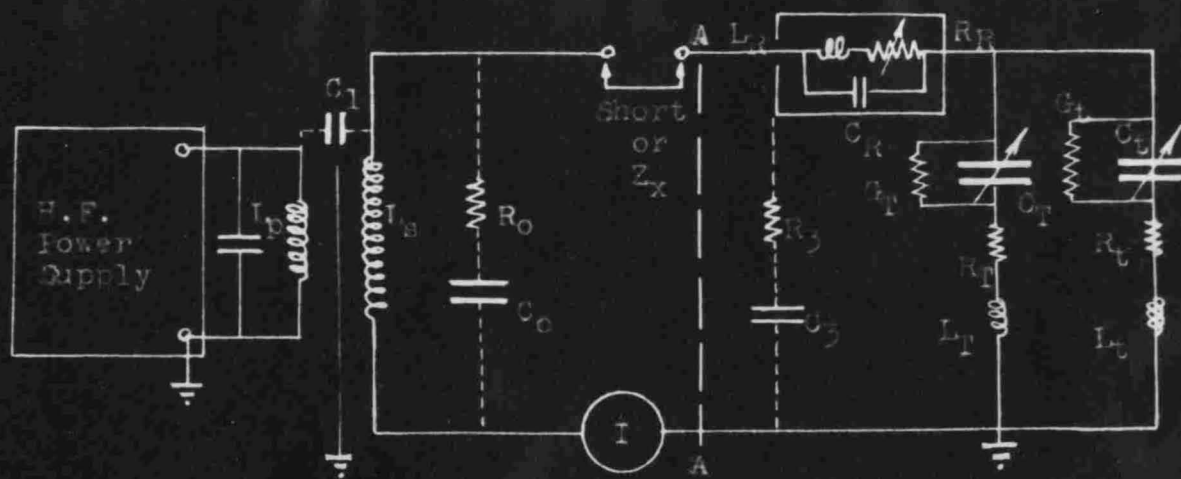
1. Substitution method.

The circuit shown in figure 28 includes the most important of the residuals that must be considered. In general the use of this circuit is limited to frequencies below approximately 30 megacycles. The simple theory indicates that there is no finite capacitive coupling between secondary and primary. Actually this is impossible to obtain. There is then a current flow through the coupling C_1 which divides into the many branches to ground yielding a loop current I which is not everywhere uniform in the secondary. This however will not affect the equations for the unknown.

It would be best if L_s were a pure inductance. Realizing that this is impossible, the type of coil selected must be carefully chosen. For work in these high frequency ranges, the Q of the coil should lie between 300 and 500. There are four sources of losses in any coil, low frequency copper loss, high frequency eddy current loss, losses due to the conductance of the equivalent stray capacitance, and losses due to the coiling effect. A log D versus log f plot of these factors reveals very clearly the suitability of a given coil for a certain frequency range.

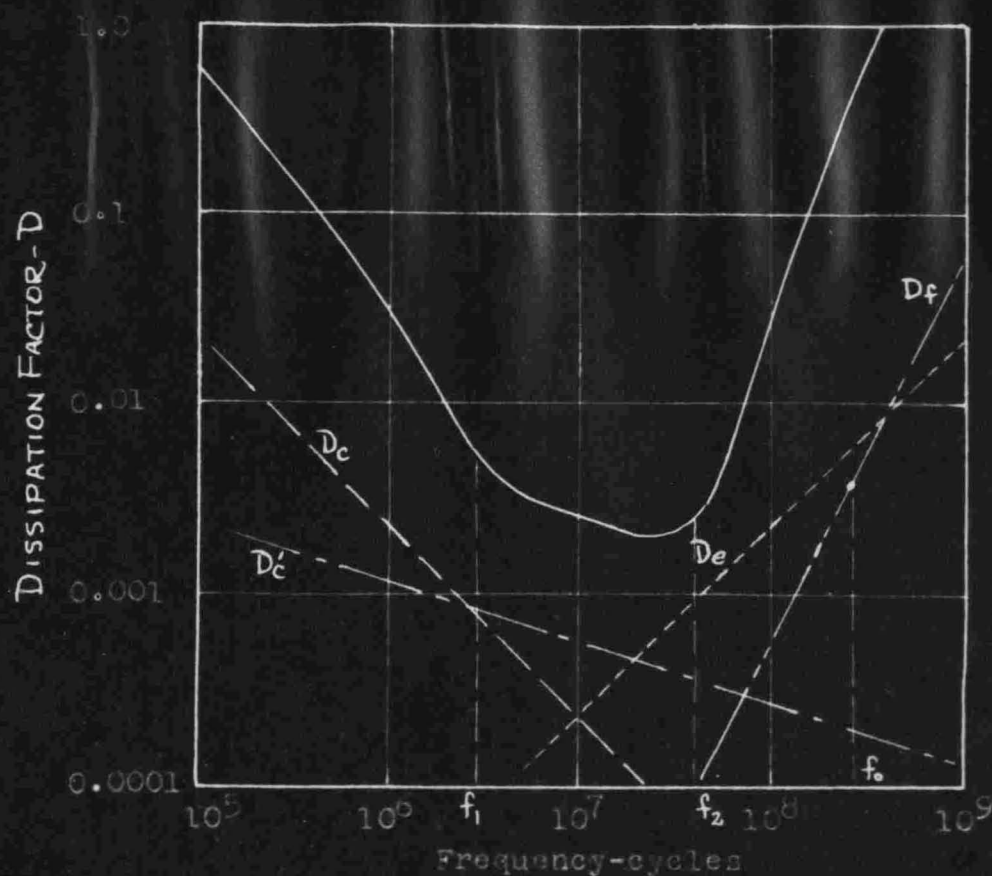
For a multiple layer coil,

$$D_c = \frac{27.0}{n a^2 N g f} = \frac{R_c}{\omega L} \quad (19)$$



Series Resonant Substitution Circuit

Fig. 28



Coil Dissipation Factor versus Frequency

Fig. 29

$$D_e = \frac{0.01845 \pi d^4 N g f}{Q^2} \times \left(\frac{B_c}{B}\right)^2 = \frac{\omega L}{R_e} \quad (20)$$

$$D_o = \omega C_o R_o \quad (21)$$

$$D_f = D_o \omega^2 L C_o = D_o \left(\frac{f}{f_o}\right)^2 \quad (22)$$

$$D_c' = \frac{3.32}{a k \sqrt{\pi f}}, \quad k = f \left(\frac{2a}{b}\right) \quad (23)$$

where D_o = Dissipation factor due to copper loss

D_c' = Dissipation factor due to coiling effect

D_e = Dissipation factor due to eddy current loss

D_f = Dissipation factor due to D_o

D_o = Dissipation factor due to natural resonant
frequency of coil

f_o = Natural resonant frequency of coil

d = Wire diameter in inches

n = Number of insulated strands

a = Mean coil diameter in inches

b = Coil length in inches

$N = \frac{b}{t} = \frac{\text{coil length}}{\text{effective wire diameter}}$

$g = f(b/c, c/a)$

Thus, by using the coil for frequencies within the range f_1 to f_2 , the highest, most uniform Q region is employed. With banked, pied coil construction, the distributed capacitance and its associated dielectric losses can be greatly reduced, increasing f_o considerably, thereby increasing the frequency at which minimum dissipation occurs.

From experimentation D_0 has been found to be approximately 0.015 for a ceramic formed coil, 0.020 for phenolic.

Aside from the part played in the determination of the coil Q , the residuals of the inductance L_S do not upset the circuit solutions.

Calculation of the circuit to the right of A-A is too involved for ready investigation. A knowledge of the procedure for measurements of unknowns will indicate what residuals must be corrected for in experimental work. With the short circuit in place and C_T set to its minimum position (100 μmf), C_t is varied to resonate the circuit as indicated by the loop current meter "A" and R is adjusted to yield a suitable meter reading. Then, with C_t unchanged, the unknown replaces the short circuit and C_T and R are readjusted to obtain the same meter reading. Thus,

$$C_x = \frac{C_{T1} C_{T2}}{C_{T2} - C_{T1}} \quad (24)$$

and
$$R_x = R_1 - R_2$$

The residuals of the trimmer capacitor element C_t will have no effect on C_x and R_x . As previously shown, C_{T1} and C_{T2} must be corrected because of the residuals associated with the standard capacitor, internally and externally across its terminals. Then

$$\frac{1}{\frac{C_{T1}}{1 - \omega^2 L C_{T1}} + C_3} = \frac{1}{\frac{C_{T2}}{1 - \omega^2 L C_{T2}} + C_3} + \frac{1}{C_x}$$

From this

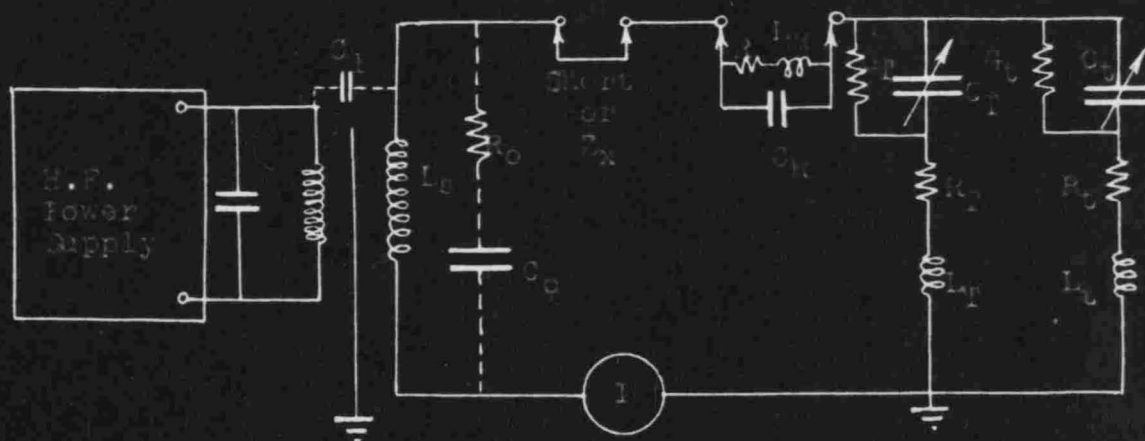
$$C_X = \frac{\left(\frac{C_{T1}}{1 - \omega^2 L C_{T1}} + C_3 \right) \left(\frac{C_{T2}}{1 - \omega^2 L C_{T2}} + C_3 \right)}{\frac{C_{T2}}{1 - \omega^2 L C_{T2}} - \frac{C_{T1}}{1 - \omega^2 L C_{T1}}} \quad (25)$$

In addition the change in the value of R in the low ohmic regions will change slightly its equivalent series reactance which must be corrected for.

2. Resistance-variation method.

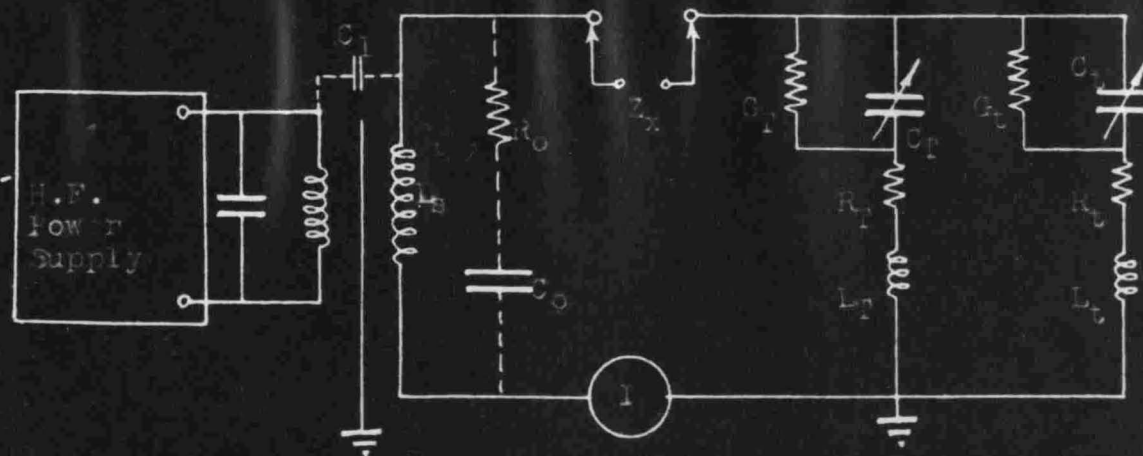
This method is very similar to the substitution method; it varies only in the manner of obtaining the unknown resistance. Instead of a continuously variable resistor, several fixed standards are used. This is actually an advantage at 100 megacycles because the fixed standards are much more predictable than the variable. The only added residuals to consider are the two contact resistances and the contact skin effect resistance. All other residuals are similar in nature and value to those in the substitution method and need not be reconsidered.

After setting C_T to a suitable value ($100 \mu\mu f$) with the short circuit in place and current resonating the circuit with C_t , insert a given value of R and noted the meter reading I_1 . Then, choosing a new value of R and leaving C_T and C_t untouched, the second meter indication is noted. In all cases of resistor substitution, the length and diameter of the resistors should be identical to insure approximately equal residuals. Then, with the nominal values R_1 and R_2 , R_{e1} and R_{e2} can be evaluated from equation 17. If R_{sec} is the series resistance of the



Series Resonant Resistance Variation Method

Fig. 30



Series Resonant Reactance Variation Method

Fig. 31

measuring circuit

$$R_{\text{sec1}} = \frac{I_2 R_{e2} - I_1 R_{e1}}{I_1 - I_2} \quad (26)$$

Replacing the short circuit with the unknown, returning to resonance with C_T and repeating the process,

$$R_{\text{sec2}} + R_x = \frac{I_4 R_{e2} - I_3 R_{e1}}{I_3 - I_4}$$

In general at lower frequencies $R_{\text{sec2}} = R_{\text{sec1}}$ but the change in setting of C_T at 100 megacycles will change its effective series resistance R_e in accordance with equation 6 and thus change the measuring circuit resistance. This change can be calculated and corrections made.

$$R_x = \frac{I_4 R_{e2} - I_3 R_{e1}}{I_3 - I_4} - \frac{I_2 R_{e2} - I_1 R_{e1}}{I_1 - I_2} - (R_{\text{sec2}} - R_{\text{sec1}}) \quad (27)$$

Ideally the unknown capacitance would be obtained from

$$C_x = \frac{(C_{T1} + C_t)(C_{T2} + C_t)}{C_{T2} - C_{T1}}$$

Actually the stray capacitance C_3 and the effective series capacitance of the fixed standard resistors must be considered and corrected for. The latter is essentially constant at 100 megacycles over the small range of resistance values necessary. These sources of error complicate the C_x equation seriously, yielding

$$C_X = \frac{C_{Re}^2 \left(\frac{C_{T1}}{1 - \omega^2 L_T C_{T1}} + C_{te} + C_3 \right) \left(\frac{C_{T2}}{1 - \omega^2 L_T C_{T2}} + C_{te} + C_3 \right)}{C_{Re} \left(\frac{C_{T2}}{1 - \omega^2 L_T C_{T2}} + C_{te} + C_3 \right) \left(C_{Re} + \frac{C_{T1}}{1 - \omega^2 L_T C_{T1}} + C_{te} + C_3 \right) - C_{Re} \left(\frac{C_{T2}}{1 - \omega^2 L_T C_{T2}} + C_{te} + C_3 \right)} \quad (28)$$

where C_{te} = Effective trimmer series capacitance,

C_{Re} = Effective resistor series capacitance,

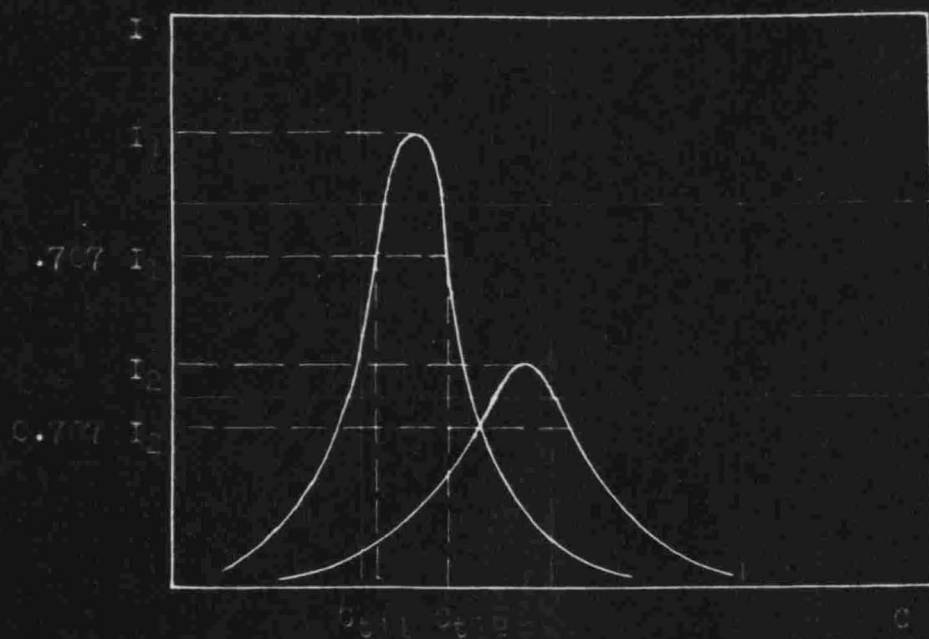
C_{T1}, C_{T2} = Initial and final tuning capacitor settings.

The value of C_{Re} can readily be determined from equation 18 and C_{te} can easily be measured by parallel substitution across C_T with the unknown replaced by the short circuit. C_3 can be estimated from the circuit construction.

3. Reactance-variation method.

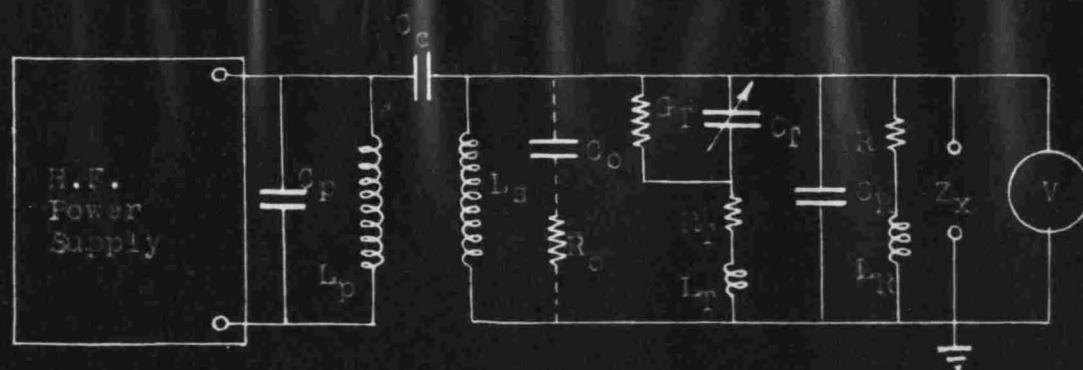
This method has the great advantage of the elimination of standard resistances and their associated errors. However measurements are not as readily made since resonance curves must be plotted for highest accuracy.

The secondary is first current resonated by varying C_T with the short circuit in place and the meter indication noted. Then, with C_T fixed, the calibrated, vernier capacitor C_t is varied on each side of resonance and the meter readings recorded for each position. With the unknown replacing the short circuit, the process is repeated. Figure 32 shows the plots of current versus vernier setting for each circuit.



Resonance Curves, constant Q and f_0 ratio

Fig. 32



Parallel Resonance Substitution Method

Fig. 33

Ideally

$$C_x = \frac{(C_T + C_{t1})(C_T + C_{t2})}{C_{t2} - C_{t1}} \quad (29)$$

and

$$R_x = \left(\frac{I_1}{I_2} - 1 \right) R_{sec} \quad (30)$$

However, taking the residuals into account and simplifying,

$$C_x = \frac{C_{t1} C_{t2} C_3 \left(\frac{1}{C_3} + \frac{1 - \omega^2 L_T C_T}{C_T} + \frac{1 - \omega^2 L_t C_{t1}}{C_{t1}} \right)}{\left(R_T + \frac{G_T}{\omega^2 C_T^2} \right) (C_{t2} - C_{t1})} \quad (29a)$$

Assuming that the residuals have little effect on the resonance curves, R_x can easily be evaluated.

$$|R_{sec}| = \left| \frac{C_{t11} + C_{t12}}{2\omega C_{t11} C_{t12}} - \frac{1}{\omega C_{t11}} \right| = \left| \frac{C_{t11} - C_{t12}}{2\omega C_{t11} C_{t12}} \right|$$

$$R_x = \left(\frac{I_1}{I_2} - 1 \right) \frac{\Delta C_{t1}}{2\omega C_{t11} C_{t12}} \quad (30a)$$

However if the change in the vernier capacitor changes the secondary resistance, the derivation for R_x becomes extremely involved. The derivation in Appendix I yields

$$R_x = \frac{1}{C_3 \left(\frac{1}{C_3} + \frac{1 - \omega^2 L_T C_T}{C_T} + \frac{1 - \omega^2 L_t C_{t1}}{C_{t1}} \right)^2} \left\{ \frac{\left(\frac{1}{C_3} + \frac{1 - \omega^2 L_T C_T}{C_T} + \frac{1 - \omega^2 L_t C_{t2}}{C_{t2}} \right)}{\frac{\omega^2 C_T C_{t2}}{1 - \omega^2 L_T (C_T + C_{t2})}} \right. \\ \left. - \beta \left(\frac{\frac{1}{C_3} + \frac{1 - \omega^2 L_T C_T}{C_T} + \frac{1 - \omega^2 L_t C_{t1}}{C_{t1}}}{\frac{\omega^2 C_T C_{t1}}{1 - \omega^2 L_T (C_T + C_{t1})}} \right) \right\} \quad (30b)$$

Except for the most accurate experimentation, equation (30b) is far too tedious.

CHAPTER V

PARALLEL RESONANCE METHODS

1. Substitution method.

The parallel resonant circuit of figure 33 includes the most important residuals to be considered. When these residuals and the errors they cause are carefully analyzed, the method can be used at frequencies up to 100 megacycles. The effect of finite capacitance coupling is to couple a certain amount of conductance into the secondary from the power source. However if the assumptions of constant frequency and linear output impedance are met, this coupled conductance will not affect the unknown equations.

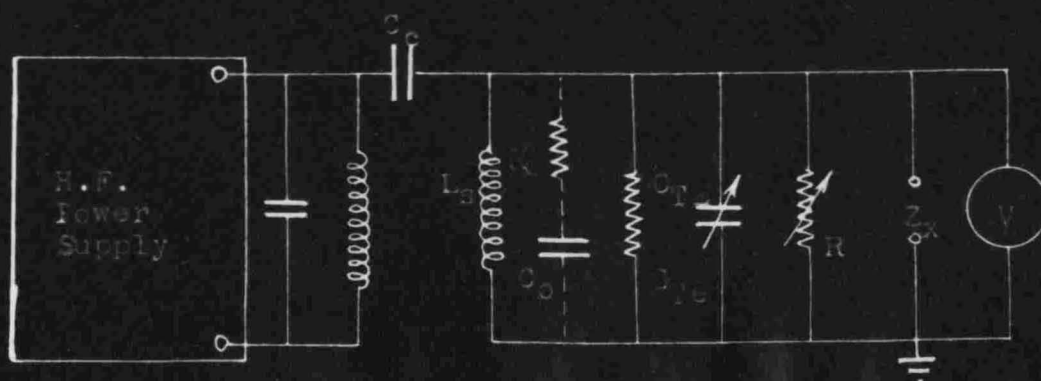
The substitution method is very simple in theory. With the unknown impedance in place, C_T is varied to resonate the circuit as indicated by the voltmeter and the meter reading is recorded. Then the unknown is replaced by the high frequency, high valued, standard variable resistor. C_T is readjusted for resonance and R is varied to give the same meter indication. From these measurements

$$C_x = C_{T2} - C_{T1} \quad (31)$$

and
$$G_x = \frac{1}{R} \quad (32)$$

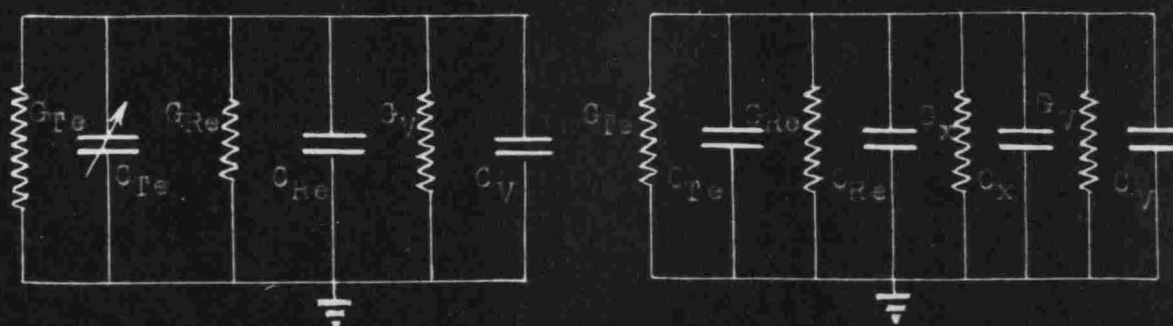
Redrawing the circuit to the right of B-B,

$$Y_{IN\ 1} = (G_{Te1} + G_x + G_v) + j\omega(C_{Te1} + C_x + C_v)$$



Parallel Resonant Conductance Variation Method

Fig. 34



Residuals, Conductance Variation Method

Fig. 35

$$Y_{IN2} = (G_{TE2} + G_{RE} + G_V) + j\omega(C_{TE2} + C_{RE} + C_V)$$

$$C_X = C_{TE2} - C_{TE1} + C_{RE}$$

$$= \frac{C_{T2}}{1 - \omega^2 L_T C_{T2}} - \frac{C_{T1}}{1 - \omega^2 L_T C_{T1}} + L_R(\omega^2 L_R C_R - 1) + C_R R^2$$

$$= \frac{C_{T2} - C_{T1}}{1 - \omega^2 L_T (C_{T1} + C_{T2})} + L_R(\omega^2 L_R C_R - 1) + C_R R^2 \quad (31a)$$

In addition to the error introduced by the effective series inductance of the tuning capacitor C_T , there is another error caused by the stray capacitance of the standard resistor. Similarly

$$G_X = G_{TE2} - G_{TE1} + G_{RE}$$

$$= G_T + R_T(\omega C_{T2})^2 - G_T - R_T(\omega C_{T1})^2 + \frac{R}{\omega^2 L_R^2 + R^2}$$

$$= R_T \omega^2 (C_{T2} - C_{T1})(C_{T2} + C_{T1}) + \frac{R}{\omega^2 L_R^2 + R^2} \quad (32a)$$

2. Conductance-variation method.

This circuit differs very little from the substitution circuit. It has the distinct advantage of eliminating the variable standard resistor and substituting in its place a fixed standard resistor. The disadvantages are an added pair of mercury cup contacts and twice as many necessary measurements. With the unknown removed and C_T adjusted for resonance at C_{T1} , if the meter is read as V_1 and V_2 with a fixed resistor first in and then out of the circuit, the circuit conductance can be derived. Ideally

$$G_{sec} = \frac{V_1}{V_2 - V_1} G_R \quad G_R = \frac{1}{R}$$

Inserting the unknown and repeating,

$$\begin{aligned} G_x &= \frac{G_{sec} (V_{1x} - V_{2x}) + G_R V_{1x}}{(V_{2x} - V_{1x})} \\ &= \frac{G_R V_1 (V_{1x} - V_{2x}) + G_R V_{1x} (V_2 - V_1)}{(V_2 - V_1)(V_{2x} - V_{1x})} \\ &= \frac{G_R (V_2 V_{1x} - V_1 V_{2x})}{(V_2 - V_1)(V_{2x} - V_{1x})} \end{aligned} \quad (33)$$

$$C_x = C_{T1} - C_{T2} \quad (34)$$

Again considering the residuals, the equations become slightly more complicated. (See figure 35).

$$\begin{aligned} V_1 \left[G_T + R_T (\omega C_{T1})^2 + \frac{R}{\omega^2 L_R^2 + R^2} + G_V \right] &= V_2 \left[G_T + R_T (\omega C_{T1})^2 + G_V \right] \\ \left[G_T + R_T (\omega C_{T1})^2 + G_V \right] &= \frac{V_1}{V_2 - V_1} \frac{R}{\omega^2 L_R^2 + R^2} \end{aligned}$$

$$\begin{aligned} \text{and } V_{1x} \left[G_T + R_T (\omega C_{T2})^2 + \frac{R}{\omega^2 L_R^2 + R^2} + G_V + G_x \right] \\ &= V_{2x} \left[G_T + R_T (\omega C_{T2})^2 + G_V + G_x \right] \\ G_x &= \frac{V_{1x}}{V_{2x} - V_{1x}} \left[G_T + R_T (\omega C_{T2})^2 + \frac{R}{\omega^2 L_R^2 + R^2} + G_V \right] \\ &\quad - \frac{V_{2x}}{V_{2x} - V_{1x}} \left[G_T + R_T (\omega C_{T2})^2 + G_V \right] \end{aligned} \quad (33a)$$

If it could be assumed that $\left[G_T + R_T (\omega C_{T2})^2 + G_V \right] = \left[G_T + R_T (\omega C_{T1})^2 + G_V \right]$, (33a) would reduce to (33). Unfortunately this equality doesn't exist; the variation in C_T is

reflected in its own effective conductance.

$$C_x = C_{Te1} - C_{Te2}$$

$$\doteq \frac{C_{T1} - C_{T2}}{1 - \omega^2 L_T (C_{T1} + C_{T2})} \quad (34a)$$

3. Susceptance variation method.

The susceptance variation method is by far the most widely used of the resonance methods. With proper precautions measurements can be made at frequencies up to 100 megacycles. and higher. Its great advantage is the elimination of the ever troublesome standard resistor. Its disadvantage, as with the reactance variation method, is the necessity of using resonance curves.

Disregarding residuals,

$$C_x = (C_{T1} + C_{t1}) - (C_{T2} + C_{t2}) \quad (35)$$

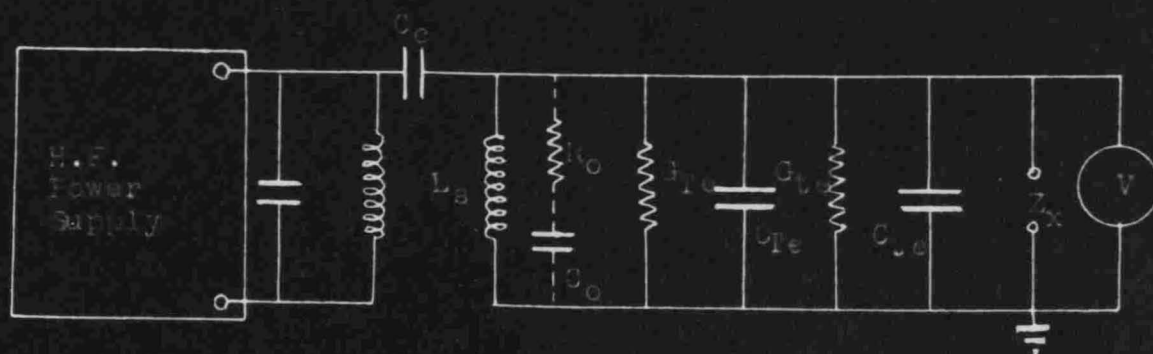
and
$$G_x = \frac{V_1 - V_2}{2} \left| \omega (C_{t11} - C_{t12}) \right| \quad (36)$$

When the residuals are considered,

$$C_x \doteq \frac{C_{T1} - C_{T2}}{1 - \omega^2 L_T (C_{T1} + C_{T2})} + \frac{C_{t1} - C_{t2}}{1 - \omega^2 L_t (C_{t1} + C_{t2})} \quad (35a)$$

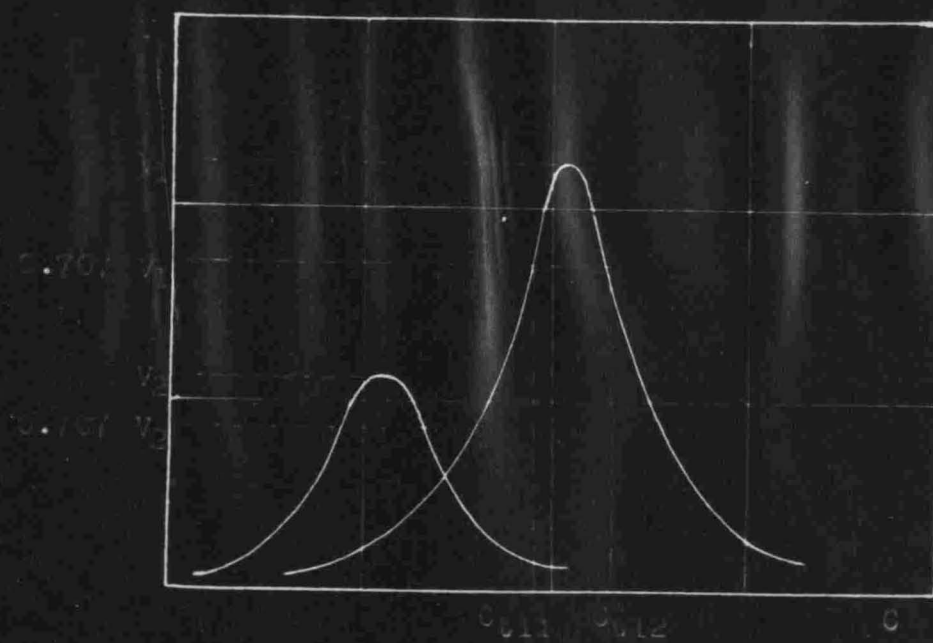
and
$$G_x = \left(\frac{V_1}{V_2} - 1 \right) (G_T + G_t + G_v) + R_T \omega^2 \left(\frac{V_1}{V_2} C_{T1}^2 - C_{T2}^2 \right) + R_t \omega^2 \left(\frac{V_1}{V_2} C_{t1}^2 - C_{t2}^2 \right) \quad (36a)$$

Equation (36a) of course demonstrates the complexity involved when the actual measuring circuit conductance cannot be assumed constant with variation of the tuning capacitor.



Parallel Resonant Susceptance Variation Method

Fig. 36



Resonance Curves, Susceptance Variation Method

Fig. 37

CHAPTER VI

THE VARIABLE DIODE CONDUCTANCE MEASURING CIRCUIT*

One of the most outstanding techniques developed in recent years is that of Weaver and McCool of the Naval Research Laboratories. It was their contention that the existing methods did not combine the best possible accuracy with the most rapid and simple techniques and least expensive equipment. With the solution of this problem as their goal, they have designed a parallel resonant, parallel substitution circuit of great versatility and high accuracy.

The unique features of this new adaption are: (1) a high degree of resolution in detecting changes in the resonant voltage of the measuring circuit, (2) the direct substitution of specimen conductance as well as capacitance, and (3) the elimination of the necessity of evaluating the total measuring circuit parameters for calibration.

The basic simplified circuit is shown in the schematic of figure 38a. The basic principle is to maintain the resonant output voltage constant before and after substitution of the unknown by simple manipulation of the tuning capacitor C_T and the equivalent diode conductance by variation of bias. Simple theory yields then, with the diode set to give an equivalent conductance G_{d1} ,

*Weaver and McCool. An improved conductance measuring circuit. Problem 39R08-44, NRL Report R-3133, June, 1947

$$G_{t1} = \text{Total circuit conductance} = G_o + G_{d1}$$

After substitution of the unknown and re-resonating,

$$G_{t2} = G_o + G_{d2} + G_x$$

Since $G_{t1} = G_{t2}$ (E_o constant),

$$G_x = G_{d1} - G_{d2} \quad (37)$$

Also, as in the parallel resonant, substitution method,

$$C_x = C_{T1} - C_{T2} \quad (38)$$

First estimation of the source of errors reveals that the precision of measurement is limited by the accuracy with which the voltmeter can be reset to E_o and by the accuracy of calibration of the equivalent diode conductance. The problem of resetting the voltmeter can best be illustrated by an example.

Let the resonant impedance of the measuring circuit be 50,000 ohms and the conductance to be measured, $0.2 \mu\text{mhos}$. What is the change in resonant voltage when the unknown is inserted?

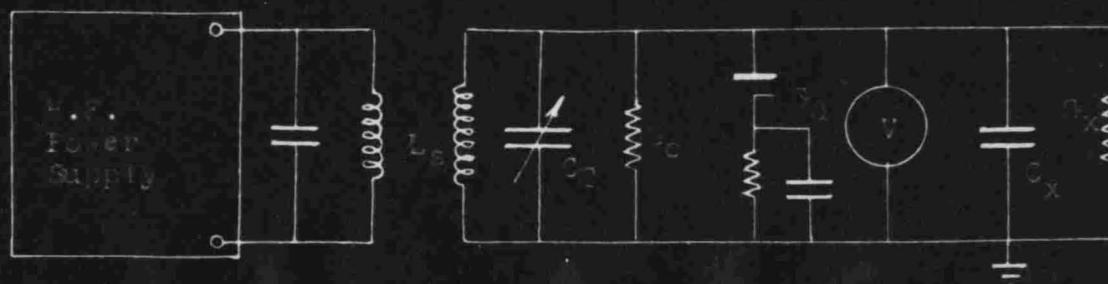
$$\frac{E_{o1}}{E_{o2}} = \frac{G_{t2}}{G_{t1}}$$

$$\frac{E_{o1} - E_{o2}}{E_{o2}} = \frac{G_{t2} - G_{t1}}{G_{t1}}$$

or

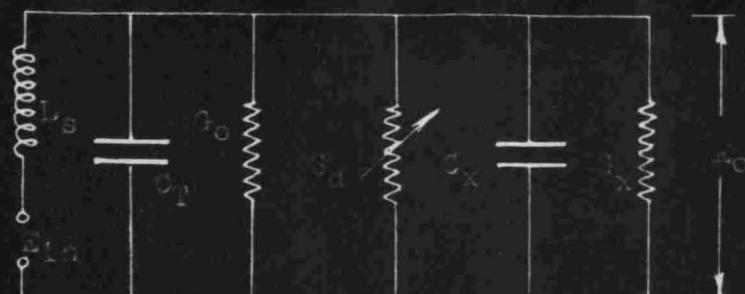
$$\frac{\Delta E_o}{E_{o2}} = \frac{\Delta G_t}{G_{t1}}$$

Substituting values,



Radio Conductance Substitution Circuit

Fig. 384



E_{in} = Equivalent constant D.C. source voltage generator.

E_o = Constant resonant output voltage.

C_1 = Resonant tuning capacitor.

C_x = Unknown capacitor.

G_o = Residual test circuit conductance.

G_d = Equivalent diode circuit conductance.

G_x = Unknown conductance.

Equivalent Conductance Substitution Circuit

Fig. 385

$$\frac{\Delta E_0}{E_{02}} = \frac{0.2 \times 10^{-6}}{20 \times 10^{-6}} = 0.01 = 1\%$$

Thus it is obvious that the error possible in resetting the voltmeter to E_0 will be of the same order of magnitude as the change in the voltage caused by the unknown. Clearly a method of indication of much greater sensitivity must be evolved. A clever means of obtaining the desired sensitivity is indicated basically in figure 39. The diode V_2 rectifies the resonant output voltage and the resulting voltage, E_{dc} , is balanced out to ground by the potentiometer arrangement across the d.c. supply, E_{bb} .

The possible error in the calibration of the variable diode conductance can be estimated from the methods of measurements used. The conductance of the diode can be measured by substitution for various known conductances or by analysis of the diode rectification characteristic. These calibrations have reportedly given results consistently agreeing to within 1 percent.

Everitt* gives the following diode circuit analysis:

$$i_p = g_p e_p \quad \text{when } e_p > 0$$

$$i_p = 0 \quad \text{when } e_p \leq 0$$

Then
$$e_p = E' \cos \omega t - E_A = E' (\cos \omega t - \cos \alpha) \quad (39)$$

$$\begin{aligned} i_p &= g_p E' (\cos \omega t - \cos \alpha) \\ &= I_0 + I_1 \cos \omega t + I_2 \cos 2(\omega t + \theta_2) \dots \quad (40) \end{aligned}$$

*Everitt, Communication Engineering. p. 427.

where I_0 = Direct current component

I_1 = Fundamental component

I_2 = Second harmonic component, etc.

However, since the parallel resonant circuit is a very low impedance to all frequency components higher than the fundamental,

$$I_p = I_0 + I_1 \cos \omega t \quad (41)$$

From Fourier analysis,

$$I_0 = \frac{g_p E'}{\pi} (\sin \alpha - \alpha \cos \alpha) \quad (42)$$

and

$$I_1 = \frac{g_p E'}{2\pi} (2\alpha - \sin 2\alpha) \quad (43)$$

Since

$$R_L = E_A / I_0 \quad \text{and} \quad R_e = E' / I_1$$

$$\frac{R_e}{R_L} = \frac{\tan \alpha - \alpha}{\alpha - \sin \alpha \cos \alpha} \quad (44)$$

Eliminating α and plotting E_A/E' against R_e/R_L will yield the universal diode rectification curve. From the plot the rectification characteristic of any series diode will give the effective conductance in terms of the applied voltage E' , the load voltage E_A , and the load resistance R_L .

A more complete schematic of the conductance measuring circuit is given in figure 41. The high frequency power supply is closely regulated so as to regulate in addition the induced voltage in the measuring circuit. The high frequency oscillator in the original work was limited to one frequency (1 megacycle) for simplicity of investigation.

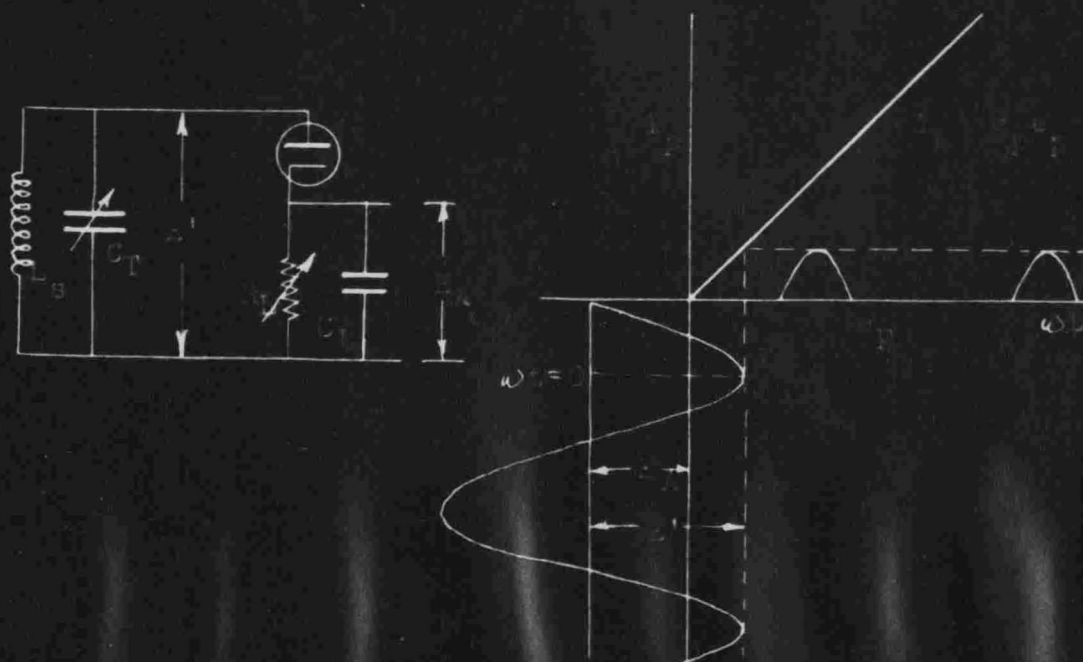
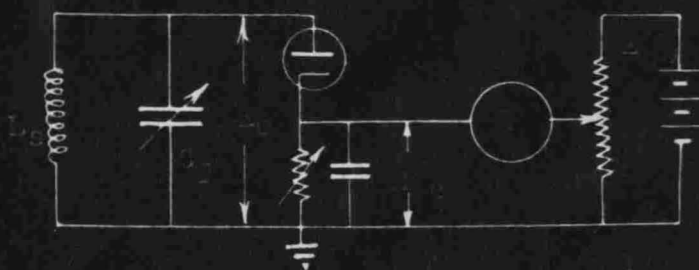
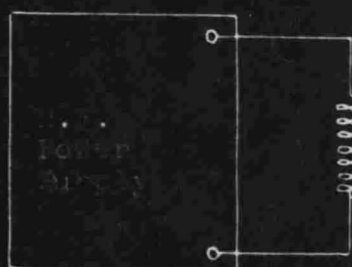
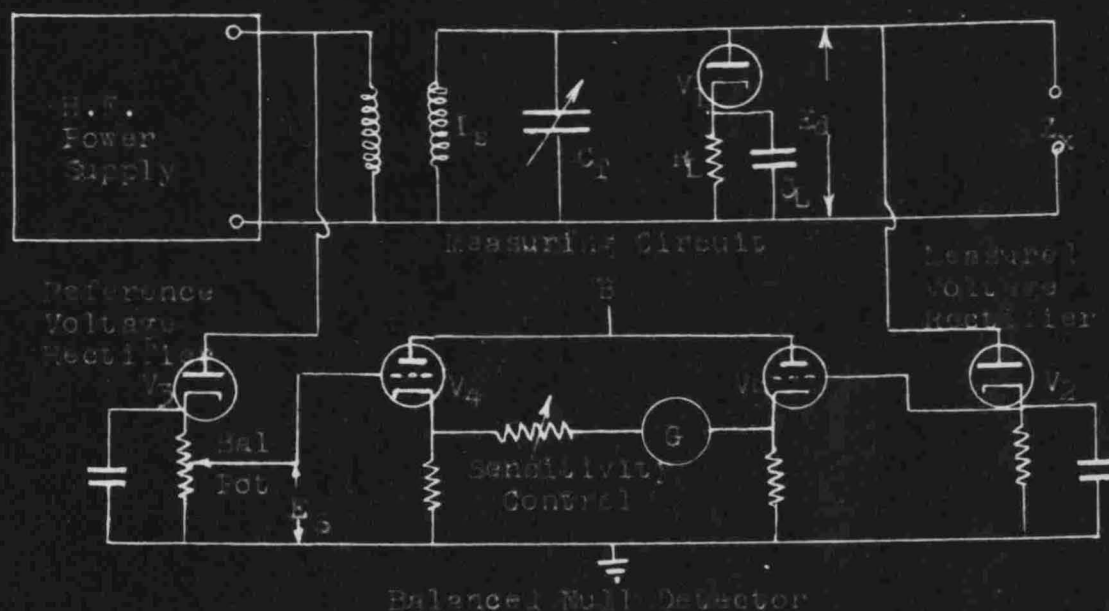


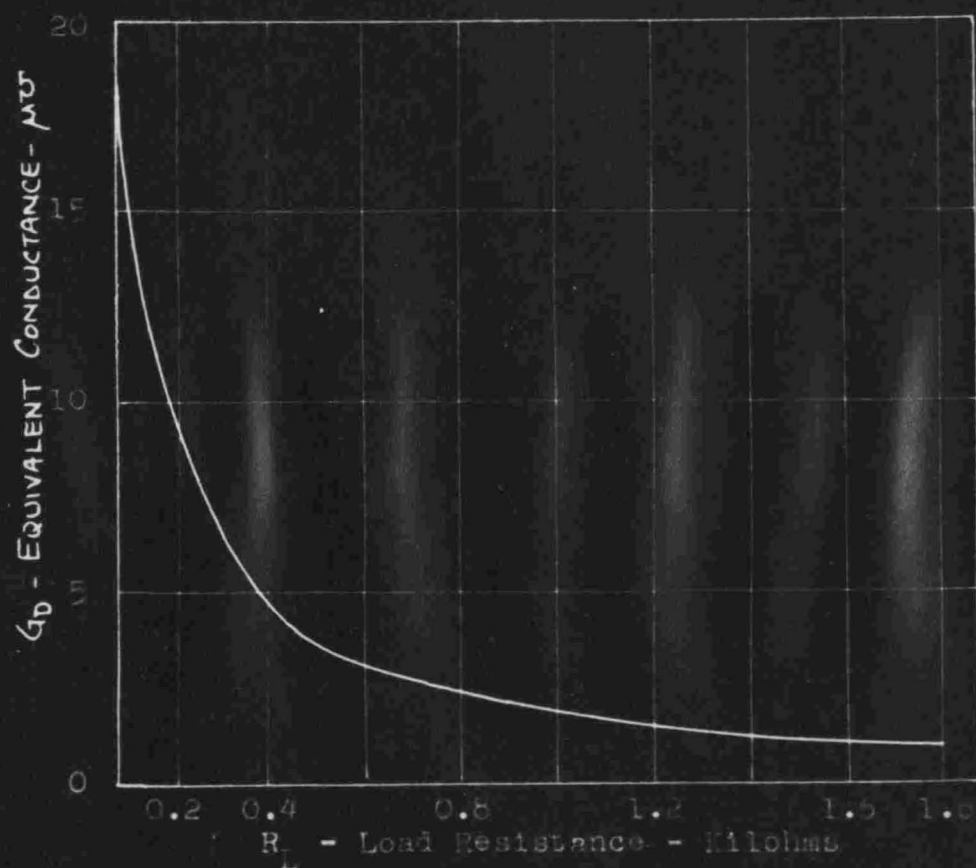
Figure 10-10. Diode Rectifier Circuit

Fig. 10-10



Conductance Meter Functional Diagram

fig. 41



Diode Circuit Conductance Calibration

fig. 42

However, such need not be the case and there is reason to believe that the method will operate successfully at 20 and possibly 100 megacycles.

The null detector is a 50-0-50 microammeter and, as a center reading meter, a voltage change of approximately one millivolt can be detected. Thus, if the resonant circuit voltage is 50 volts rms, one part in 50,000 can be detected. Very simply then, with the unknown out of the circuit, the high frequency regulated supply is rectified in V_3 and the resonant output voltage in V_2 ; the resulting d.c. voltages are applied to the grids of V_4 and V_5 respectively and balanced by means of the balancing potentiometer. With the unknown in place and the balance untouched, the output of the measuring circuit at resonance can be controlled by the variable conductance and can be reset to the initial value when the null detector is zeroed. Thus the duplication should be precise to within 0.2 percent. Experimentation shows the duplication to be within 0.3 to 0.5 percent.

In order to exploit the extremely high sensitivity of the method, the overall conductance calibration curve (figure 42) must be exploded into more accurately readable plots. The method used to accomplish this is explained in Appendix II.

The diode circuit has a definite voltage coefficient such that a change in applied voltage shifts the calibration. Figure 43 demonstrates the percent change in diode circuit conductance versus R_L . The greatest shift is in the high

conductance end of the calibration. Weaver and McCool pointed out that, when measuring low values of conductance, the low end of the calibration is used and in this region tube aging, tube replacement, and voltage coefficient effects are negligible.

An example of the performance of this circuit is the measurement of the power factor of dry air which was found to be 0.000002 ± 50 percent.

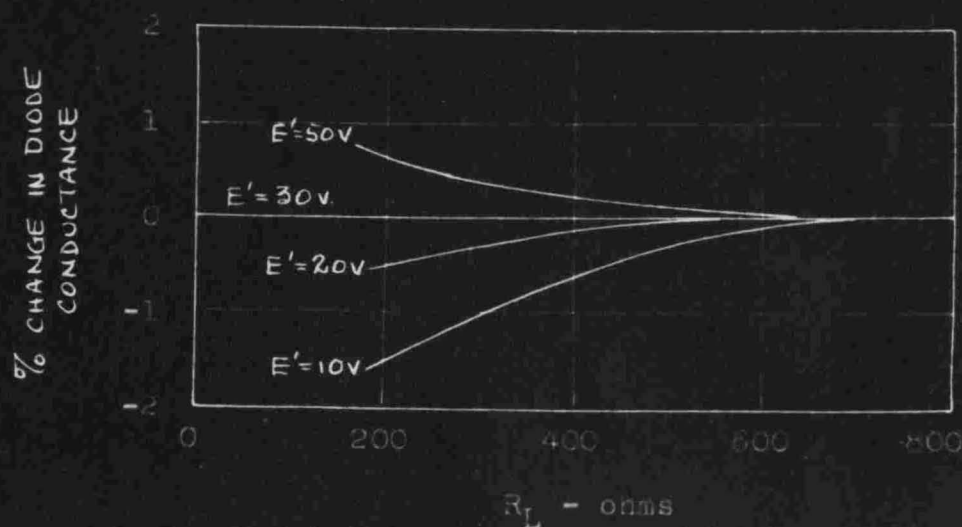
There has been no evaluation of some of the more important residuals of this conductance circuit and it would be of interest to determine their effect. From figure 44

$$\begin{aligned} G_0 + G_{Te1} + G_{D1} &= G_0 + G_{Te2} + G_{D2} + G_X \\ G_X &= (G_{Te1} - G_{Te2}) + (G_{D1} - G_{D2}) \\ &= [G_T + R_T(\omega C_{T1})^2 - G_T - R_T(\omega C_{T2})^2] + (G_{D1} - G_{D2}) \\ &= R_T \omega^2 (C_{T1}^2 - C_{T2}^2) + (G_{D1} - G_{D2}) \quad (37a) \end{aligned}$$

Similarly, $C_0 + C_{Te1} + C_{Pk} = C_0 + C_{Te2} + C_{Pk} + C_X$

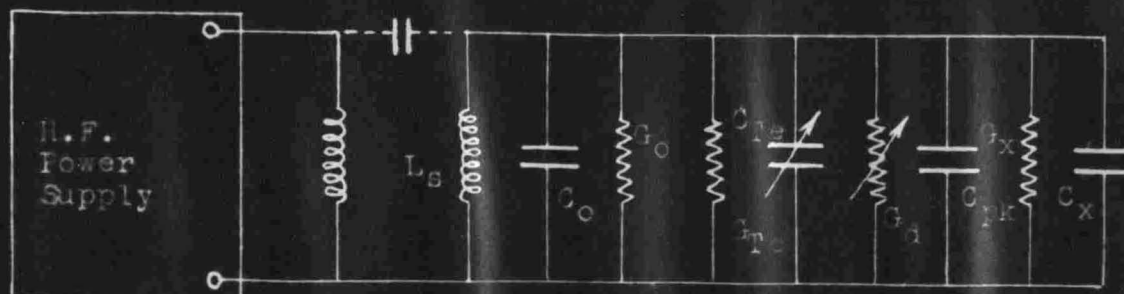
$$C_X = \frac{C_{T1} - C_{T2}}{1 - \omega^2 L_T (C_{T1} + C_{T2})} \quad (38a)$$

Obviously, in measuring low valued conductances, the residual series resistance of the standard capacitor must be considered. It is equally as necessary that the effect of the residual series inductance, L_T , must be appreciated and corrected for as frequency increases.



Diode Circuit Voltage Coefficient

Fig. 43



Residuals, Conductance Measurement Circuit

Fig. 44

CHAPTER VII

NULL METHODS

1. Impedance bridge.

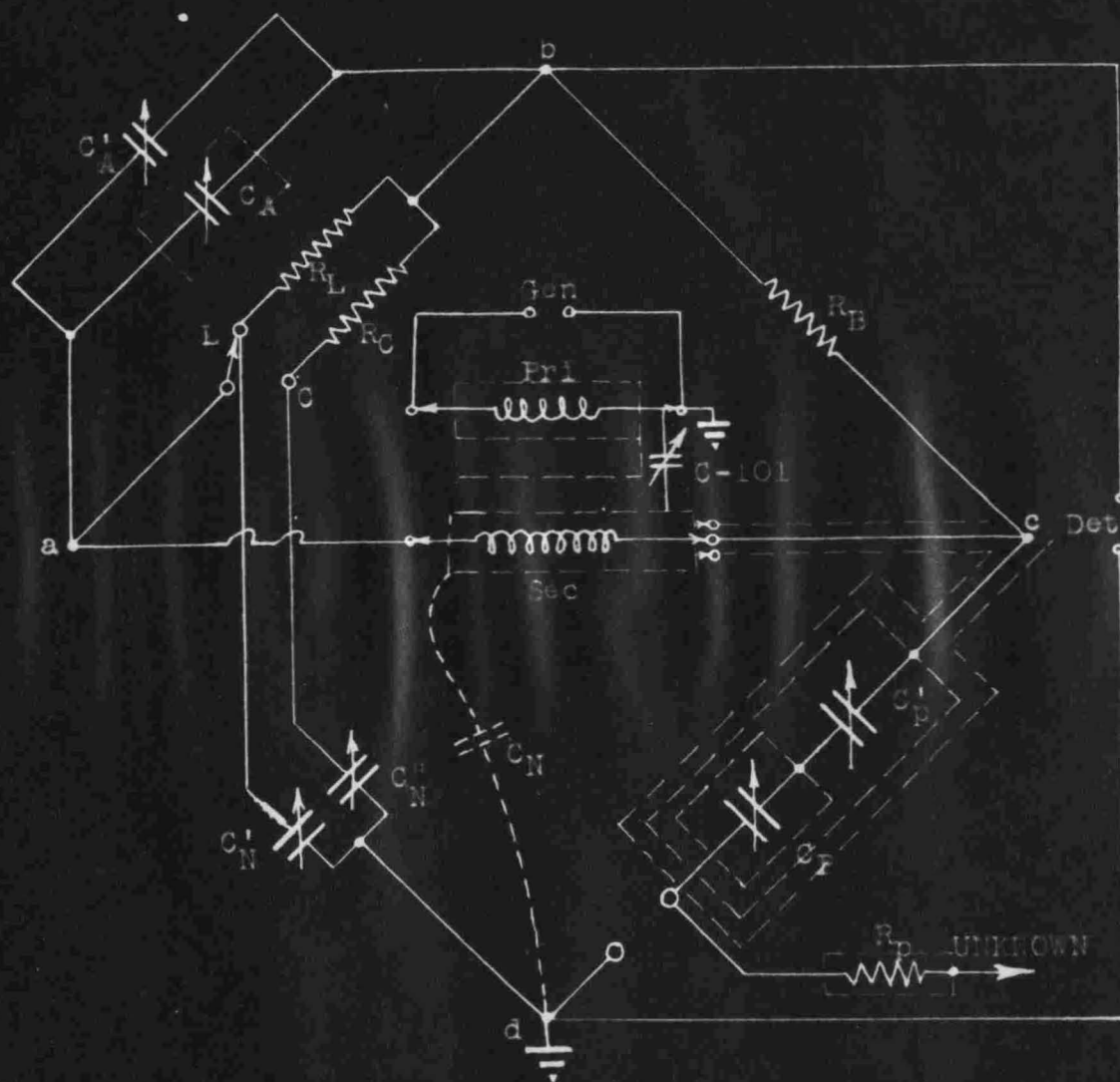
The equal arm impedance type bridge has been found unsuitable for commercial development for use at 10 to 100 megacycles. It depends upon the use of a precision variable resistor in its standard arm. As explained in Chapter III, it has been common experience that the design and development of such a precision variable resistor satisfactory for general use at very high frequencies is a difficult problem not yet solved.

Until such a resistor is available, the impedance bridge must yield to slightly more complex bridge circuits.

2. Modified Schering bridge.

The General Radio Company manufactures three impedance bridges which are representative of the modified Schering bridge. They are the 916-AL, the 916-A and the 1601 which cover the frequency ranges 50 kilocycles to 5 megacycles, 400 kilocycles to 60 megacycles, and 20 to 140 megacycles respectively. Only the 916-A and the 1601 will be considered here.

The basic circuit of the 916-A is shown in figure 5; the more complete schematic in figure 45. With the added C_p and C_A the resistance dial, calibrated directly in ohms, and the reactance dial, calibrated at any one frequency,



General Radio 910-A Radio Frequency Bridge

Fig. 45

can be set to any position desired and an initial balance obtained. Thus with the switch in the L position, C_p can be set to zero (maximum capacitance) for maximum range of inductance measurement; or, in the C position, C_p can be set at 5000 ohms (minimum capacitance) for greatest range of capacitance measurement. C_N is composed almost entirely of the stray capacitance between the outer C_p - C'_p shielding and the grounded case. The addition of the very small trimmers, C'_N and C''_N , is to insure that the total capacitance from the left hand junction to ground is equal for both positions of the L-C switch.

The initial balance conditions, with the UNKNOWN terminals short circuited with the appropriate lead, are

$$R_p = R_B \frac{C_{A1}}{C_N} \quad (45)$$

$$\frac{1}{j\omega C_{p1}} = \frac{R_B}{R_A} \frac{1}{j\omega C_N}$$

where C_{A1} represents the total capacitance of the settings of C_A and C'_A , and C_{p1} represents the total series capacitance of C_p and C'_p . With the unknown capacitor to be measured in position (C_{p1} would have been set at 5000 ohms), the bridge is rebalanced to a null by varying only C_A and C_p . C'_A and C'_p remain fixed. Thus

$$R_p + R_x = R_B \frac{C_{A2}}{C_N} \quad (46)$$

$$\frac{1}{j\omega C_{p2}} + \frac{1}{j\omega C_x} = \frac{R_B}{R_A} \frac{1}{j\omega C_N}$$

$$R_x = R_B \frac{(C_{A2} - C_{A1})}{C_N} \quad (46)$$

$$X_x = \frac{1}{\omega} \left(\frac{1}{C_{p2}} - \frac{1}{C_{p1}} \right)$$

From equations 46 and 47 it is apparent that R_A is necessary only for the initial balance; it does not appear in the unknown equations. Two such resistors are necessary to provide the range of initial balance as the L-C switch and the initial setting of C_p are changed. R_B is a fixed, essentially non-reactive, precision resistor. R_p is a necessary balancing resistor and, as will be shown later, is most conveniently located externally to the bridge.

It is convenient now to consider the effects of the various residual parameters upon the impedance of the four bridge arms. Starting with the bridge arm "a-b", R_A is not and need not be a precision resistor. If the tuning of C'_A can overcome the reactances of the residual series inductance and parallel capacitance of R_A , the resistor will function satisfactorily. Any stray capacitance from point "b" to ground falls across the detector and is ineffective; Stray capacitance from "a" to ground is across the "d-a" arm and is equalized for the two switch positions by the choice of C'_N and C''_N .

The residuals of the precision capacitor, C_A , will contribute seriously to erroneous results if not accounted

for. The effective series inductance due to the current distribution in the capacitor structure causes the terminal capacitance to vary from the static capacitance C_A by

$$C = \frac{C_A}{1 - \omega^2 L C_A}$$

The effect of this on the resistance (equation 46) is to yield values that are too low, especially at high frequency. Therefore it is quite necessary to correct the C_A resistance dial readings at the upper frequency limit. The residual series resistance component of the capacitor introduces a parallel conductance $R(\omega C_A)^2$ across R_A and modifies the reactance balance equation by

$$X_x = \frac{1}{\omega} \left(\frac{1}{C_{p2}} - \frac{1}{C_{p1}} \right) - R \frac{\omega C_A R_x}{R_B} (2R_p + R_x) \quad (48)$$

The error, never greater than about one ohm, causes the reactive result to be slightly more inductive than it should be. The residual conductance, G_A , of C_A falls across R_A and effects no incremental error since it is independent of rotor setting.

The precision resistor in the "b-c" arm must be as nearly non-reactive as possible. The 916-A uses a 0.7 mil, "straight wire" manganin resistor which is equivalent to a pure 270 ohms resistance in parallel with approximately 0.4 μf up to 60 megacycles. This residual capacitance causes an error in the reactive equation (again in the inductive direction) as follows:

$$X_x = \frac{1}{\omega} \left(\frac{1}{C_{p2}} - \frac{1}{C_{p1}} \right) - \frac{\omega C_B}{G_B} R_x \quad (49)$$

The error caused by this residual capacitance is of the same order of magnitude as the variation in results obtained by changing the position of the ungrounded connector to the unknown.

Again, any capacitance from point "b" to ground is un harmfully across the detector. Point "c" has essentially no stray capacitance to ground due to the completeness of the shielding.

Since stray capacitances are so deleterious in the arm "c-d", a very complete shielding system has been designed. The capacitance between point "c" and the outer shield is thrown across the generator and rendered harmless. That capacitance between the center and inner shield is in parallel with C'_p and affects the initial balance only. The inner shield isolates the variable stray C due to the position of the C_p rotor from the trimmer C'_p .

It would be advantageous to locate R_p within the bridge structure. However, so doing would introduce harmful strays which would upset the balance. For instance, if R_p were connected in series with C'_p within the inner and center shield, the capacitance between these two shields would fall across this series combination. Therefore, as C'_p is varied, the equivalent resistance would also change. This would limit the range over which initial balance could be obtained. It has been found most practical to locate R_p

external to the bridge and to shield it such that the capacitance to ground of the lead from C_p to the unknown is negligibly small.

Another source of error is the residual conductance (constant with setting) of C_p . This conductance, which increases with frequency, is equivalent to a series resistance which varies inversely with frequency and inversely with the square of the capacitance setting. This error becomes insignificant at the high frequencies of which we are interested.

The bridge arm "d-a" is to all aspects a pure capacitance even at these high frequencies. Its residuals are so small that they have no observable effects on bridge balancing.

The General Radio Catalog L avers that the accuracy of reactance measurements up to 50 megacycles is $\pm(2 \text{ percent} + 1 \text{ ohm} + 0.0008 Rf)$ where R is the measured resistance in ohms and f is the frequency in megacycles. It is difficult to tell whether this is an overall percentage accuracy which takes every reactance-affecting residual into account. Suppose that a precision air capacitor set at $500 \mu f$ with 0.02 ohms series residual resistance is to be measured at 50 megacycles. What percentage error may be expected? Substituting in the formula

$$\begin{aligned}\Delta X &= \pm(0.1273 + 1.0 + 0.0008 \times 0.02 \times 50) \\ &= \pm(1.1281) \text{ OHMS}\end{aligned}$$

But

$$X = \frac{1}{2\pi 50 \times 10^{-6} \times 500 \times 10^{-12}} = 6.365 \text{ OHMS}$$

This is an apparent possible error of 17.7 percent. It would be wise in high frequency problems to disregard such a statement of accuracy and instead to calculate from formulii and correction graphs supplied the effects of the residuals.

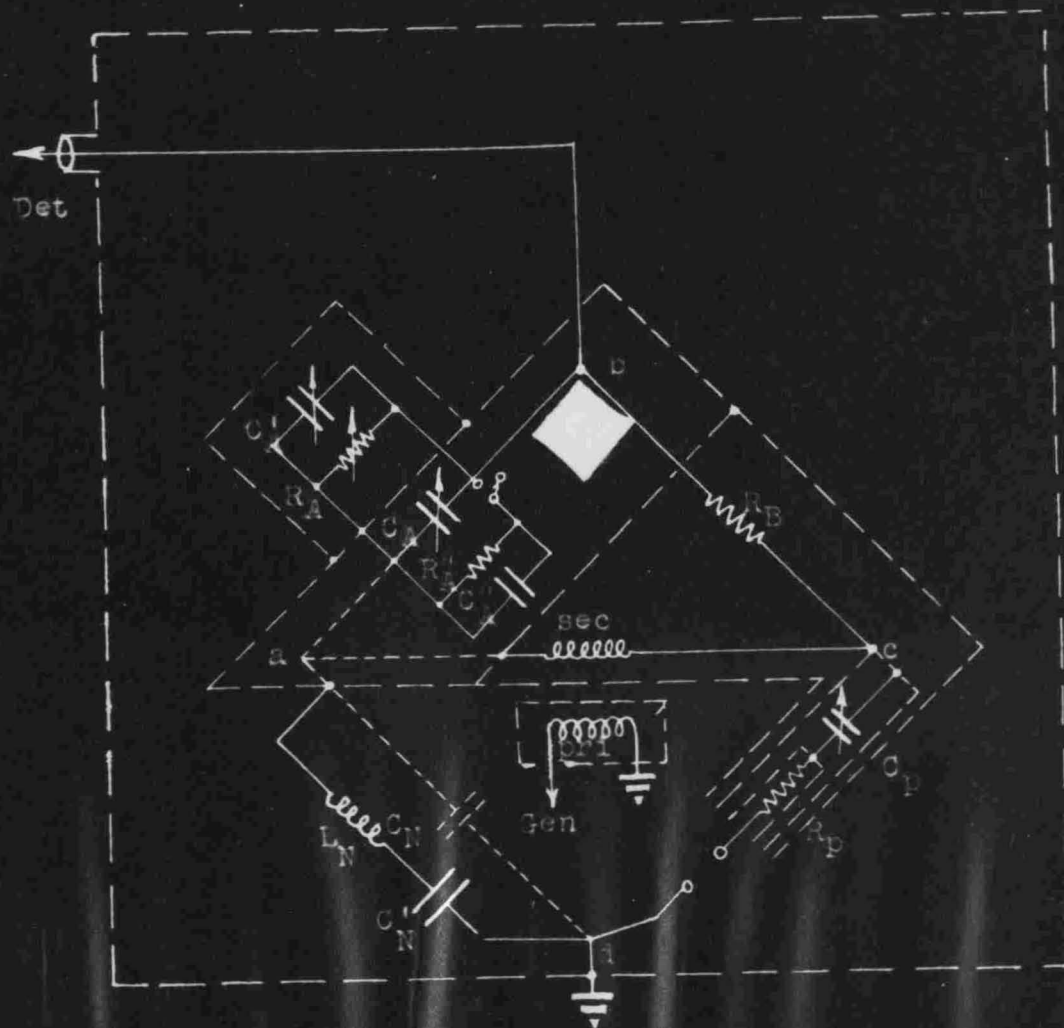
The stated accuracy for resistance measurements at 50 megacycles is $\pm(1 \text{ percent} + 0.1 \text{ ohms})$. The 0.1 ohms correction is possibly attributed to inability to read the dial to greater precision.

3. The 1601 VHF bridge.

This bridge is basically a higher frequency version of the 916-A. Physically it is much smaller since the size of the components parts becomes less as frequency is increased. But the bridge circuit is a modified Schering type (see figure 5) and the balance conditions are the same as equations 45, 46 and 47. The complete circuit diagram is shown in figure 46.

In the design of this bridge from its predecessor, it was found in some cases that common inductances as small as 0.5×10^{-9} henries and stray capacitances as small as 0.05×10^{-12} farads between elements that can not be completely shielded from one another, cause appreciable error. Again, by examining each bridge arm individually, the effects of the residuals can best be evaluated.

As in the 916-A, the residuals in the arm "a-b" in



General Radio 16C1 VHF Bridge

Fig. 40

R_A and C'_A have no effect on the accuracy of measurement. However they do seriously affect the initial balance conditions and may so modify the arm impedances that balancing is impossible. This is especially true when the bridge is set up to measure a large capacitive reactance. It was found that the condition could be improved by inserting in parallel with R_A a fixed resistor and capacitor. (C'_p has been eliminated and R_A has been made adjustable to accomplish the initial reactive balance). Shielding of this arm eliminates stray capacitances to ground and to other arms.

The resistance capacitor, C_A , here, as in the 916-A, is not a pure reactance. Its series inductance, L_A , affects the terminal capacitance as before where

$$C_{Ae} = \frac{C_A}{1 - \omega^2 L_A C_A}$$

The effective incremental change in capacitance would then be

$$\Delta C_{Ae} = \Delta C_A [1 + \omega^2 L_A (2C_A + \Delta C_A)] \quad (50)$$

From this equation it can be seen that the deviation is proportional to the square of the frequency and is dependent upon the magnitude of the measured resistance. In order to reduce this residual error, it was found that an inductive circuit added in parallel with C_N would offer some compensation. This increases the effective value of

C_N by

$$C_{Ne} = (C_N + C'_N) \left[1 + \omega^2 L_N \frac{C_N'^2}{C_N + C'_N} \right] \quad (51)$$

Since

$$R_x = R_B \frac{\Delta C_{Ae}}{\Delta C_{Ne}}$$

it is possible by correctly selecting L_N and C'_N to correct to a first order approximation for the error caused by C_A .

The remaining deviation is given by

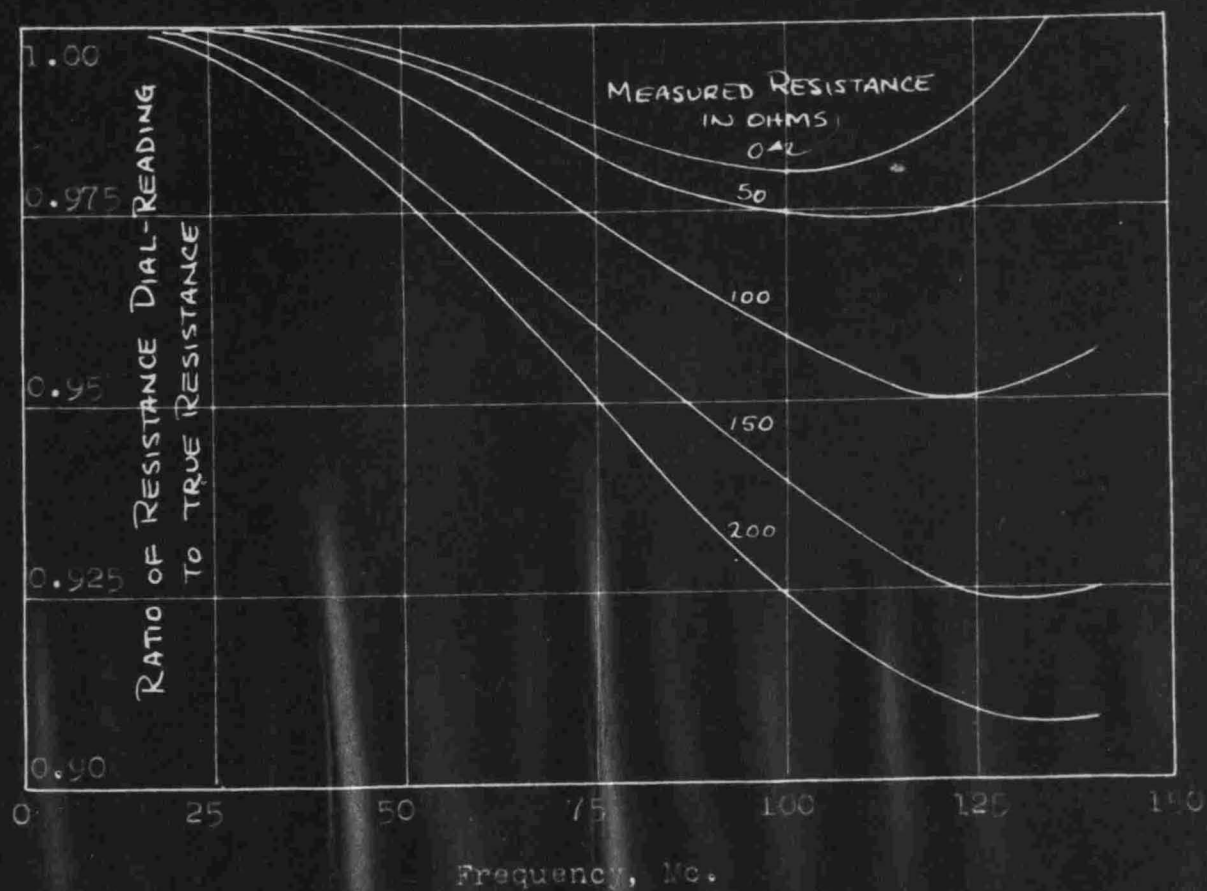
$$\Delta R_x = \frac{\omega^2 L_A}{R_B} (C_N + C'_N) R_m^2 \quad (52)$$

where R_m is the dial reading. Figure 47 shows the magnitude of the correction which still must be applied to the resistance dial reading.

In the precision resistance arm "b-c", any reactive residuals will cause errors in the reactance measurement. However, if the constants of the equivalent circuit of the resistor (figure 22) can be chosen or designed such that

$$R = \sqrt{\frac{L}{C}} \quad (53)$$

then the series reactive component of the arm will be small at frequencies which are an appreciable fraction of the natural resonant frequency. In order to push up this operating frequency level, L and C must be made small. It was necessary to go to a cylindrical palladium and palladium oxide resistor fitted with threaded end caps to eliminate wire connectors to accomplish this end. With this construction, $C = 0.31 \mu\mu f$ and $L = 0.017 \mu h$ and $R = 240$ ohms.



Effect of Inductance in Resistance
Capacitor, C_A , on Indicated Resistance

Fig. 47

The UNKNOWN arm "c-d" is of finite length and must have a residual inductance, L_p . However, since a series substitution method is employed and since the residual inductance is there in both initial and final positions, it does not affect measured reactance. The initial balance is affected in that R_A must be increased to overcome the effective rise of C_p due to this inductance.

Because C'_p is no longer mused, the balancing resistor R_p can now become integrated internally. The tri-shield is similar to that used in the 916-A. Any stray capacitance between the inner shield and the lead to the UNKNOWN terminal is directly across R_p . This has no effect on the bridge accuracy and simply inserts an effective series capacitance which may be beneficial. If the capacitance across R_p is such that

$$R_p = \sqrt{\frac{L_p}{C_{Rp}}} \quad (54)$$

then the compensation for L_p is very good at frequencies which are an appreciable fraction of the equivalent resonant frequency.

Stray capacitance between the inner and middle shield falls directly across C_p and need only be considered in the initial calibration. Strays between the middle and outer shields are across the generator and exert no effect. A capacitance exists between the lead from R_p to the UNKNOWN terminal and the middle and outer shields. By using a very small diameter lead and by proper shield design, these

capacitances can be made negligibly small.

There are no noteworthy residuals to be considered in the "d-a" arm. From figure 46 it can be seen that all bridge components except the generator and C_N are enclosed in a common shield connected to the bridge at point "a". C_N is the capacitance of this shield to ground and is not a physical capacitor. It is paralleled by the L_N-C_N' compensation circuit.

One other residual capacitance need be considered. It is that between the UNKNOWN terminal and ground and is of the order of $1.05 \mu\mu\text{f}$. Since it is in parallel with the unknown capacitance it must be corrected for,

The 1601 is still under experimental test and is not yet on the market. It is expected that the accuracy of reactive measurements will be within 5 percent at 140 megacycles and the accuracy of resistive measurements will be within 2 percent.

4. Twin-T method.

The General Radio Company version of the parallel-T circuit is the 821-A Twin-T impedance measuring circuit. It utilizes the very convenient parallel substitution method of inserting the unknown. Balance conditions for the circuit (figure 6) are as follows:

$$G_L - R\omega^2 C' C'' \left(1 + \frac{G}{C'''}\right) = 0 \quad (55)$$

$$C_B + C' C'' \left(\frac{1}{C'} + \frac{1}{C''} + \frac{1}{C'''}\right) - \frac{1}{\omega^2 L} = 0 \quad (56)$$

The unknown is then given by:

$$G_x = \frac{R\omega^2 C' C''}{C'''} (C_{G2} - C_{G1}) \quad (57)$$

$$B_x = \omega (C_{B1} - C_{B2}) \quad (58)$$

As was briefly discussed in the introduction, stray capacitances from points "a" and "c" to ground, from "a" to "b", "b" to "c" and "d" to "a" are ineffective or can be included in the initial calibration. Capacitance across the standard resistor, if of the correct order of magnitude, can be beneficial and capacitances from "a" to "c" must be minimized or eliminated by shielding.

As with any bridge circuit, it must be possible to get an initial balance and to have a reasonable range of measurement of conductance and susceptance at any frequency within the range of the instrument. The measuring circuit from "b" to ground is primarily a parallel tuned circuit. The coil L is shunted by an effective capacitance C_B plus $(C' + C'' + C' C'' / C''')$. Because it is not feasible to use just one coil over the frequency range of 0.5 to 30 megacycles, provision is made to switch in one of four coils which cover the range in four steps. Since C' , C'' and C''' are essentially fixed capacitors, an additional parallel capacitor system must supplement C_B in order that an initial balance may be obtained for any setting. This parallel supplement consists of four fixed capacitors inserted by push button control and small trimmer. Similarly the conductance measuring capacitor, C_G , must be paralleled

with a coarse and fine trimmer capacitor in order that C_G may be set at zero initially for any measurement.

From equation 57 it can be seen that the conductance range increases with the square of the frequency; this would yield a very undesirable 3600:1 ratio of conductance ranges over the frequency range 0.5 to 30 megacycles. If, while switching coils, C' and C'' or C''' are switched simultaneously, any desired ratio may be obtained. This circuit has been designed to give a range of 0-100 mhos at 1 megacycle, 0-300 at 3 megacycles, 0-1000 at 10 megacycles and 0-3000 at 30 megacycles.

It is vital at these high frequencies to reduce to a minimum the inductance of the wiring. It is especially necessary that the capacitors C' , C'' and C''' and the resistor R be connected as closely as possible with as large a diameter connection as is feasible. Therefore, copper strap has been used and the lead lengths are all less than one inch. In addition the junction points "b" and "d" must be located as close to the capacitor plates of C_B and C_G as possible. This will minimize the series inductances in the measuring circuits.

The most critical element in the circuit is C_B which is a 100-1100 $\mu\mu\text{f}$ capacitor utilizing double end-feed of the rotor stack through 48 current entry points and double feed to the stator stack. A further gain in reduction of influential residuals has been realized by making the capacitor a 3-terminal network. This is natural since there must

be one stator lead to the ungrounded UNKNOWN terminal and one stator lead to the junction point "b" in addition to the ground lead. An equivalent circuit of this construction is shown in figure 48.

The effect of L' is to insert a positive reactance in series with the unknown. The effective admittance, Y'_x , measured at b' is then

$$Y'_x = G'_x + jB'_x = \frac{G_x}{(1 - \omega L' B_x)^2} + j \frac{B_x}{1 - \omega L' B_x} \quad (59)$$

which will differ from the true value ($Y_x = G_x + jB_x$) in either direction depending upon the sense of the unknown susceptance.

The effect of the common inductance L_c is again that of increasing the effective capacitance over the static value in accordance with

$$C_{Be} = \frac{C_B}{1 - \omega^2 L_c C_B}$$

This effective increase in capacitance makes the measured value of susceptance as read from the dial less than the true value as shown in equation 60.

$$B'_x = \omega (C_{Be1} - C_{Be2}) = \frac{\omega (C_{B1} - C_{B2})}{1 - \omega^2 L_c (C_{B1} + C_{B2})} \quad (60)$$

Here again the error encountered is proportional to the sum of the errors at the initial and final settings of C_B . The 3-terminal construction makes both L_c and L' about one-

half of the inductance that would be measured in a 2-terminal capacitor. This twofold reduction therefore decreases the errors of equation 60.

Since the susceptance from point b' is the same for both initial and final settings, the inductance L" has no effect on the susceptance measurement. However, since the circuit actually measures conductance from point b" to ground, L" will affect the conductance measurement. It can

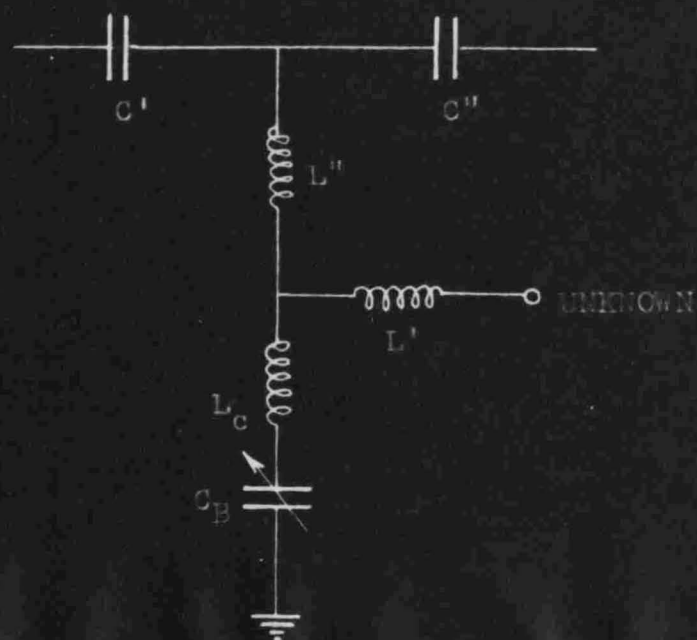
$$G_y'' = \frac{G_x}{(1 - \omega^2 L'' C_{Be1})^2 (1 - \omega L' B_x)^2} \quad (61)$$

be seen that L" always makes the conductance measured too high while L' will either make it too high or too low, depending upon the sense of B_x.

To be complete the equivalent circuit (48) must include the ohmic losses of the inductances and the shunt conductance of the capacitor. R' and R" are so small that they have negligible effect on the accuracy of measurement. The conductance is independent of rotor setting and is therefore constant for initial and final settings. But the common resistance R_c introduces a conductance term, (R_c ω² C_{Be}²), which is dependent upon the square of the rotor setting and which will be a source of error in the conductance measurement. This error will be

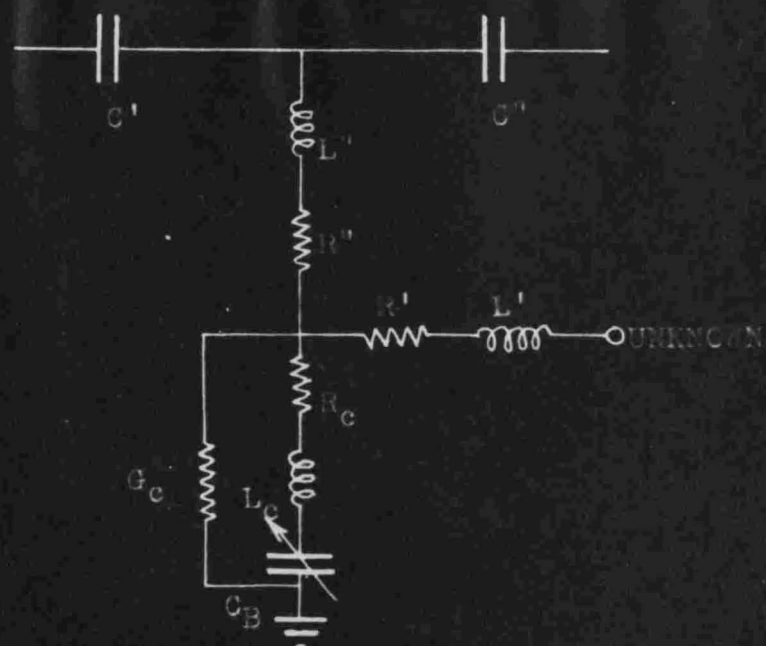
$$\Delta G = R \omega^2 (C_{Be1}^2 - C_{Be2}^2) \quad (62)$$

Thus, when measuring an unknown capacitance, this error



Approximate Equivalent Circuit of C_B

Fig. 48



Approximate Equivalent Circuit of C_B

Including Residual Losses

Fig. 49

will tend to make the measured conductance value too small.

These residual parameters which are associated with the capacitor C_B are the limiting factors determining the upper frequency limit at which accurate measurements may be made. Experimental results yield the following average values:

$$L' = 6.8 \times 10^{-9} \text{ henries}$$

$$L'' = 3.15 \times 10^{-9} \text{ henries}$$

$$L_C = 6.1 \times 10^{-9} \text{ henries}$$

$$R_C = 0.026 \text{ ohms.}$$

CHAPTER VIII

CONCLUSIONS

It is felt, with no further explanation necessary, that the series and parallel resonant substitution methods and the resistance-variation and conductance-variation methods (excluding the variable diode conductance measuring circuit) should be eliminated from the consideration of circuits to be used for highly accurate, high frequency measurement of capacitors. Further, it seems logical to assume that the remaining methods will, with due regard for their frequency limitations, yield results of consistent accuracy. By taking all the necessary precautions indicated, these methods should yield results accurate to within 2 percent in the frequency range from 30 to 140 megacycles.

Obviously the null methods offer the easiest means of measurement. However, they also pose a more difficult problem in the control of residuals. There is little that can be done to alter the commercial bridge equipments. The lower capacitance limit of the 916-A at 50 megacycles is approximately $35 \mu\mu\text{f}$ while that of the 1601 is about $8 \mu\mu\text{f}$ at 100 megacycles, that of the 821-A Twin-T is zero at 30 megacycles. The resistance dials of the 916-A and the 1601 and the conductance dial of the 821-A would be of little use in measuring very low loss capacitors.

On the other hand, the two remaining resonance methods will yield very good results even for low loss capacitors.

Inherently they are slower, more tedious methods because of the necessary plotting but the control that may be exercised over the residual parameters is much greater. The reactance-variation circuit lends itself to the measurement of low series resistance components and the susceptance-variation to the measurement of low parallel conductance components.

The variable diode conductance measuring circuit, if further study reveals that it can be made to operate at 100 megacycles, will probably surpass these more conventional methods for ease and accuracy of measurement.

BIBLIOGRAPHY

1. Breit, G. The distributed capacity of inductance coils. Phys. Rev. 2nd ser, 17:649, June, 1921.
2. Brown, S. L. and Colby, M. Y. Electrical measurements at radio frequencies. Phys. Rev. 2nd ser, 29:717, May, 1927.
3. Brown, S. L., Weibusch, C. F. and Colby, M. Y. The high frequency resistance of a Bureau of Standards type air condenser. Phys. Rev. 2nd ser, 29:887, June, 1927.
4. Burke, C. T. Substitution method for the determination of resistance of inductors and capacitors at radio-frequencies. Trans. A.I.E.E. 46:482, 1927.
5. Easton, I. G. Corrections for residual impedances in the Twin-T. Reprint from General Radio Experimenter.
6. Easton, I. G. Impedance bridges assembled from laboratory parts. General Radio Company, 1943.
7. Everitt, W. L. Communication Engineering. New York and London, McGraw-Hill. 1937.
8. Field, R. F. Connection errors in capacitance measurements. General Radio Experimenter. 12 No. 8, January, 1938.
9. Field, R. F. Increased accuracy for the precision condenser. General Radio Experimenter. 22 No. 1, June, 1947.
10. Field, R. F. and Sinclair, D. B. A method for determining residual inductance and resistance of a variable air condenser at radio frequencies. Reprint from Proc. I.R.E. 24 No. 2, February, 1936.
11. General Radio Company. Operating instructions for type 821-A Twin-T impedance measuring circuit. Form 566-C.
12. General Radio Company. Operating and maintainance instructions for type 916-A radio frequency bridge. Form 567-H.
13. General Radio Company. Operating instructions for type 916-AL radio frequency bridge. Form 708-A.
14. Hartshorn, L. Radio frequency measurements by bridge and resonance methods. New York, John Wiley & Sons, Inc., 1943.

15. Hartshorn, L. and Ward, W. H. The measurement of the permittivity and power factor of dielectrics at frequencies from 10^4 to 10^8 cycles per second. Proc. Wireless Section I.E.E. (London). 12:6, March, 1937.
16. Howe, G. W. O. Editorial in Wireless Engineering. June, 1935.
17. Howe, G. W. O. Editorial in Wireless Engineering. August, 1935.
18. Jackson, W. The analysis of air condenser loss resistance. Proc. I.R.E. 22:957-963, August, 1934.
19. Maibauer, A. E. and Taylor, T. S. The variation of the resistance of condensers with dial setting at radio frequency. Phys. Rev. 2nd ser, 27:251, February, 1926.
20. Sayce, A. A simple method of measuring capacity and high frequency loss of a condenser. Jour. Sci. Instr. 3:116, January, 1926.
21. Simmonds, J. C. Apparatus for measurements on balanced-pair cables in the range 10-200 mc/s. Proceedings of the Wireless Section. 92 III 20:282, December, 1945.
22. Simmonds, J. C. Tuned circuit, parallel resistance substitution apparatus for measurements on balanced-pair cables at frequencies up to 10 mcps. Proceedings of the Wireless Section. 92 III 18:120, June, 1945.
23. Sinclair, D. B. A high-frequency model of the precision condenser. General Radio Experimenter. 13 Nos. 5 and 6, October, 1938.
24. Sinclair, D. B. A radio-frequency bridge for impedance measurements from 400 kilocycles to 60 megacycles. Proc. I.R.E. November, 1940.
25. Sinclair, D. B. High-frequency measurements. Radio-Electronic Engineering. December, 1945-January, 1946.
26. Sinclair, D. B. Impedance measurements on broadcast antennas. Communications. June and July, 1939.
27. Sinclair, D. B. Parallel-resonance methods for precise measurements of high impedances at radio-frequencies and a comparison with the ordinary series-resonance methods. Reprint from Proc. I.R.E. 26 No.12, December, 1938.

28. Sinclair, D. B. The Twin-T, a new type of null instrument for measuring impedance at frequencies up to 30 megacycles. Proc. I.R.E. July, 1940.
29. Smiley, G. Eccentricity effects of precision rotary devices. General Radio Experimenter. 22 No. 8, January, 1948.
30. Soderman, R. A. A new bridge for impedance measurements at frequencies between 50 kilocycles and 5 megacycles. General Radio Experimenter. 23 No. 10, March, 1949.
31. Soderman, R. A. A v-h-f bridge for impedance measurements at frequencies between 20 and 140 megacycles. General Radio Company.
32. Soderman, R. A. Measurements on i-f transformers with the 916-A r-f bridge. General Radio Experimenter. 23 No. 8, January, 1949.
33. Soderman, R. A. Sensitivity of the type 916-A radio frequency bridge. General Radio Experimenter. 22 No. 8, January, 1948.
34. Sutton, G. W. A method for the determination of the equivalent resistance of air condensers at high frequencies. Proc. Phys. Soc. (London). 41:126, February, 1929.
35. Taylor, P. B. Method for measurement of high resistance at high frequencies. Proc. I. R. E. 20:1802-1806, November, 1932.
36. Tuttle, W. N. Bridge-T and parallel-T null circuits for measurements at radio frequencies. Proc. I.R.E. January, 1940.
37. Weaver, E. O. and McCool, W. A. An improved conductance measuring circuit. Naval Research Laboratories. R-3133, June, 1947.
38. Weyl, C. N. and Harris, S. A method of measuring at radio frequencies the equivalent series resistance of condensers intended for use in radio receiving circuits. Proc. I.R.E. 13:109-150, February, 1925.
39. Wilmotte, R. M. The comparison of the power factors of condensers. Wireless Engineer and Experimental Wireless. 6:656, December, 1929.
40. Wilmotte, R. M. A quick and sensitive method of measuring condenser losses at radio-frequencies. Jour. Sci. Instr. 5:369, December, 1928.

APPENDIX I

RESIDUALS, REACTANCE VARIATION METHOD

The following laborious derivation is typical of much of the work in the field of residuals as encountered in high frequency measuring circuits. See figure 53.

$$I_1 \left[\frac{-j\frac{1}{\omega C_3}(R_{Te} - j\frac{1}{\omega C_{Te}})(R_{Te} - j\frac{1}{\omega C_{Te1}})}{(R_{Te} + R_{Te}) - \frac{j}{\omega}(\frac{1}{C_3} + \frac{1}{C_{Te}} + \frac{1}{C_{Te1}})} + j\omega L \right]$$

$$= I_2 \left[R_x - j\frac{1}{\omega C_x} + \frac{-j\frac{1}{\omega C_3}(R_{Te} - j\frac{1}{\omega C_{Te}})(R_{Te} - j\frac{1}{\omega C_{Te2}})}{(R_{Te} + R_{Te}) - \frac{j}{\omega}(\frac{1}{C_3} + \frac{1}{C_{Te}} + \frac{1}{C_{Te2}})} + j\omega L \right]$$

Rationalizing the denominators,

$$I_1 \left\{ - \frac{\frac{1}{\omega^2 C_3}(R_{Te} + R_{Te}) \left(\frac{R_{Te}}{C_{Te}} + \frac{R_{Te}}{C_{Te1}} \right) - \frac{1}{\omega^2 C_3} \left(\frac{1}{C_3} + \frac{1}{C_{Te}} + \frac{1}{C_{Te1}} \right) (R_{Te} R_{Te} - \frac{1}{\omega^2 C_{Te} C_{Te1}})}{(R_{Te} + R_{Te})^2 + \frac{1}{\omega^2} \left(\frac{1}{C_3} + \frac{1}{C_{Te}} + \frac{1}{C_{Te1}} \right)^2} \right.$$

$$\left. - \frac{j}{\omega} \left[\frac{\left(\frac{R_{Te} + R_{Te}}{C_3} \right) \left(R_{Te} R_{Te} - \frac{1}{\omega^2 C_{Te} C_{Te1}} \right) + \frac{1}{\omega^2 C_3} \left(\frac{1}{C_3} + \frac{1}{C_{Te}} + \frac{1}{C_{Te1}} \right) \left(\frac{R_{Te}}{C_{Te}} + \frac{R_{Te}}{C_{Te1}} \right)}{(R_{Te} + R_{Te})^2 + \frac{1}{\omega^2} \left(\frac{1}{C_3} + \frac{1}{C_{Te}} + \frac{1}{C_{Te1}} \right)^2} \right] + j\omega L \right\}$$

$$= I_2 \left\{ R_x - \frac{\frac{1}{\omega^2 C_3}(R_{Te} + R_{Te}) \left(\frac{R_{Te}}{C_{Te}} + \frac{R_{Te}}{C_{Te2}} \right) - \frac{1}{\omega^2 C_3} \left(\frac{1}{C_3} + \frac{1}{C_{Te}} + \frac{1}{C_{Te2}} \right) (R_{Te} R_{Te} - \frac{1}{\omega^2 C_{Te} C_{Te2}})}{(R_{Te} + R_{Te})^2 + \frac{1}{\omega^2} \left(\frac{1}{C_3} + \frac{1}{C_{Te}} + \frac{1}{C_{Te2}} \right)^2} \right.$$

$$\left. - \frac{j}{\omega} \left[\frac{1}{C_x} + \frac{\left(\frac{R_{Te} + R_{Te}}{C_3} \right) \left(R_{Te} R_{Te} - \frac{1}{\omega^2 C_{Te} C_{Te2}} \right) + \frac{1}{\omega^2 C_3} \left(\frac{1}{C_3} + \frac{1}{C_{Te}} + \frac{1}{C_{Te2}} \right) \left(\frac{R_{Te}}{C_{Te}} + \frac{R_{Te}}{C_{Te2}} \right)}{(R_{Te} + R_{Te})^2 + \frac{1}{\omega^2} \left(\frac{1}{C_3} + \frac{1}{C_{Te}} + \frac{1}{C_{Te2}} \right)^2} \right] + j\omega L \right\}$$

At resonance

$$\frac{I_1}{I_2} \left[\frac{-\frac{1}{\omega^2 C_3} (R_{Te} + R_{Tc}) \left(\frac{R_{Tc}}{C_{Te}} + \frac{R_{Tc}}{C_{Te1}} \right) - \frac{1}{\omega^2 C_3} \left(\frac{1}{C_3} + \frac{1}{C_{Te}} + \frac{1}{C_{Te1}} \right) \left(R_{Te} R_{Tc} - \frac{1}{\omega^2 C_{Te} C_{Te1}} \right)}{(R_{Te} + R_{Tc})^2 + \frac{1}{\omega^2} \left(\frac{1}{C_3} + \frac{1}{C_{Te}} + \frac{1}{C_{Te1}} \right)^2} \right] =$$

$$\left[R_x - \frac{\frac{1}{\omega^2 C_3} (R_{Te} + R_{Tc}) \left(\frac{R_{Tc}}{C_{Te}} + \frac{R_{Tc}}{C_{Te2}} \right) - \frac{1}{\omega^2 C_3} \left(\frac{1}{C_3} + \frac{1}{C_{Te}} + \frac{1}{C_{Te2}} \right) \left(R_{Te} R_{Tc} - \frac{1}{\omega^2 C_{Te} C_{Te2}} \right)}{(R_{Te} + R_{Tc})^2 + \frac{1}{\omega^2} \left(\frac{1}{C_3} + \frac{1}{C_{Te}} + \frac{1}{C_{Te2}} \right)^2} \right]$$

$$R_x = \frac{1}{\omega^2 C_3} \left[\frac{(R_{Te} + R_{Tc}) \left(\frac{R_{Tc}}{C_{Te}} + \frac{R_{Tc}}{C_{Te2}} \right) - \left(\frac{1}{C_3} + \frac{1}{C_{Te}} + \frac{1}{C_{Te2}} \right) \left(R_{Te} R_{Tc} - \frac{1}{\omega^2 C_{Te} C_{Te2}} \right)}{(R_{Te} + R_{Tc})^2 + \frac{1}{\omega^2} \left(\frac{1}{C_3} + \frac{1}{C_{Te}} + \frac{1}{C_{Te2}} \right)^2} \right]$$

$$- \beta \frac{(R_{Te} + R_{Tc}) \left(\frac{R_{Tc}}{C_{Te}} + \frac{R_{Tc}}{C_{Te1}} \right) - \left(\frac{1}{C_3} + \frac{1}{C_{Te}} + \frac{1}{C_{Te1}} \right) \left(R_{Te} R_{Tc} - \frac{1}{\omega^2 C_{Te} C_{Te1}} \right)}{(R_{Te} + R_{Tc})^2 + \frac{1}{\omega^2} \left(\frac{1}{C_3} + \frac{1}{C_{Te}} + \frac{1}{C_{Te1}} \right)^2} \right]$$

At 100 megacycles

$$R_x = \frac{1}{C_3 \left(\frac{1}{C_3} + \frac{1}{C_{Te}} + \frac{1}{C_{Te1}} \right)^2} \left[\frac{\left(\frac{1}{C_3} + \frac{1}{C_{Te}} + \frac{1}{C_{Te2}} \right)}{\omega^2 C_{Te} C_{Te2}} - \beta \frac{\left(\frac{1}{C_3} + \frac{1}{C_{Te}} + \frac{1}{C_{Te1}} \right)}{\omega^2 C_{Te} C_{Te1}} \right]$$

$$= \frac{1}{C_3 \left(\frac{1}{C_3} + \frac{1 - \omega^2 L_T C_T}{C_T} + \frac{1 - \omega^2 L_t C_{t2}}{C_{t2}} \right)^2} \left[\frac{\left(\frac{1}{C_3} + \frac{1 - \omega^2 L_T C_T}{C_T} + \frac{1 - \omega^2 L_t C_{t2}}{C_{t2}} \right)}{\omega^2 C_T C_{t2}} \right]$$

$$- \beta \frac{\left(\frac{1}{C_3} + \frac{1 - \omega^2 L_T C_T}{C_T} + \frac{1 - \omega^2 L_t C_{t2}}{C_{t2}} \right)}{\omega^2 C_T C_{t1}} \left[\frac{1}{(1 - \omega^2 L_T C_T)(1 - \omega^2 L_t C_{t1})} \right]$$

Similarly

$$\frac{1}{C_X} = \frac{\frac{R_T + \frac{G}{\omega^2 C_T^2} \left(\frac{C_{t2} - C_{t1}}{C_{t1} C_{t2}} \right)}{C_3}}{\left(\frac{1}{C_3} + \frac{1 - \omega^2 L_T C_T}{C_T} + \frac{1 - \omega^2 L_t C_{t1}}{C_{t1}} \right)}$$

APPENDIX II

EXPANSION OF THE DIODE CIRCUIT CALIBRATION

$$R_e = R_L \frac{\tan \alpha - \alpha}{\alpha - \sin \alpha \cos \alpha} \quad (1)$$

As R_L approaches infinity,

$$\frac{R_e}{R_L} \rightarrow 0.5 \quad (2)$$

In the calibration process the ratio R_e/R_L is obtained directly from the universal diode curve. The range of values for this ratio is very limited, extending to 0.58 when $R_L = 10^5$ ohms and V_1 6H6. Let

$$R_T = R_e - \frac{R_L}{2} = \left(\frac{R_e}{R_L} - \frac{1}{2} \right) R_L \quad (3)$$

R_T is a fictitious resistance representing the difference between the equivalent diode circuit resistance and $R_L/2$, the limiting value of R_e as R_L approaches infinity. By plotting R_T against R_L and rearranging the equation 3,

$$R_e = \frac{R_L}{2} + R_T = \frac{1}{G_d} \quad (4)$$

Thus from equation 4, the diode circuit conductance can be computed. It is made up of two parts, (1) $R_L/2$ computed from the measured value of the load resistance and (2) R_T which is read from a highly expanded curve. (See figure 51). Figure 52 is a specimen exploded conductance curve.

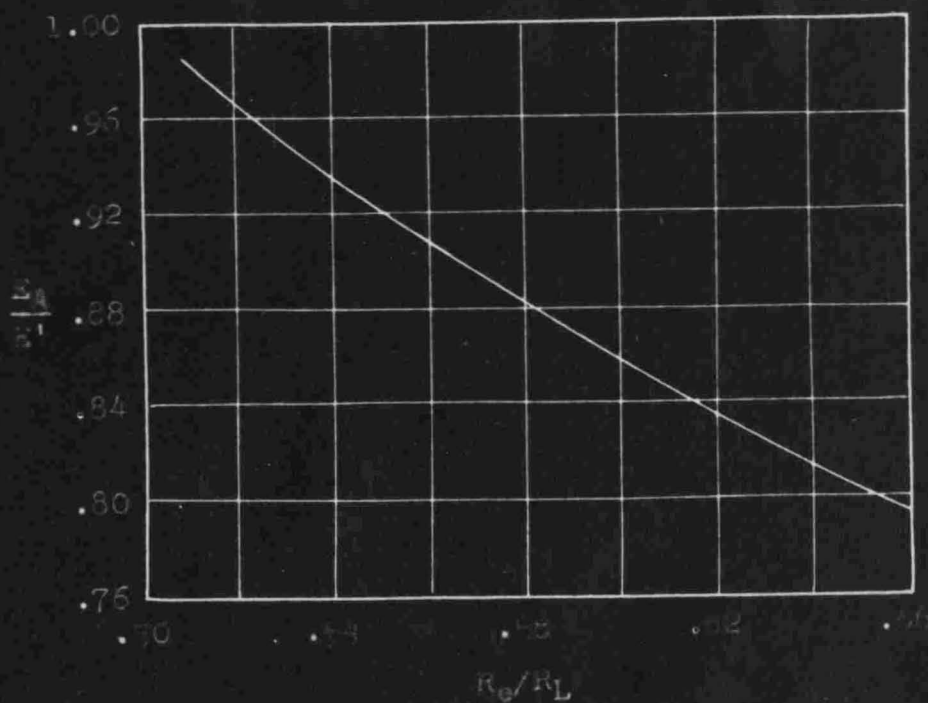
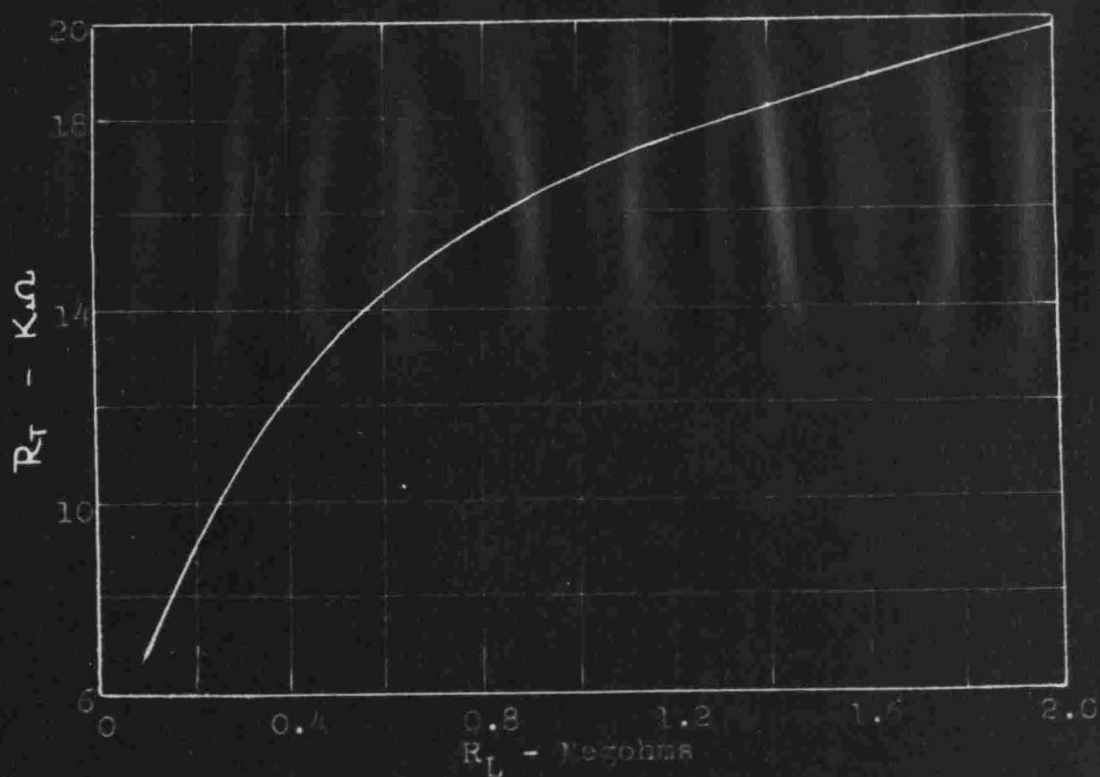
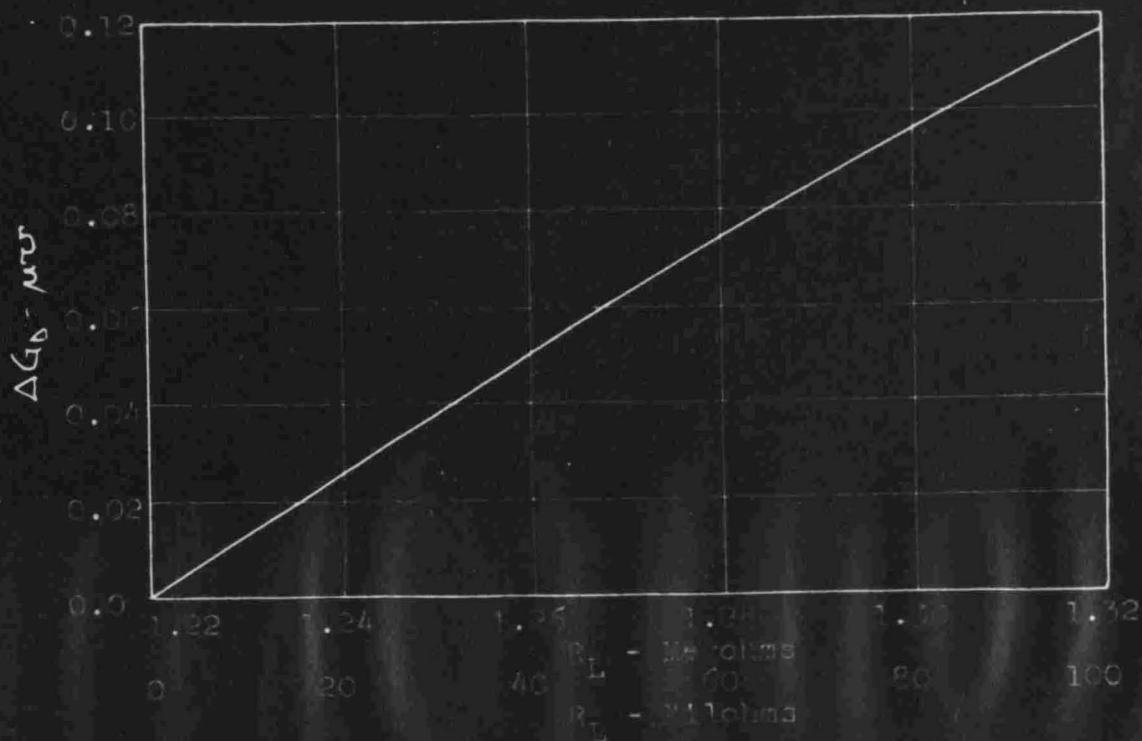


Fig. 50



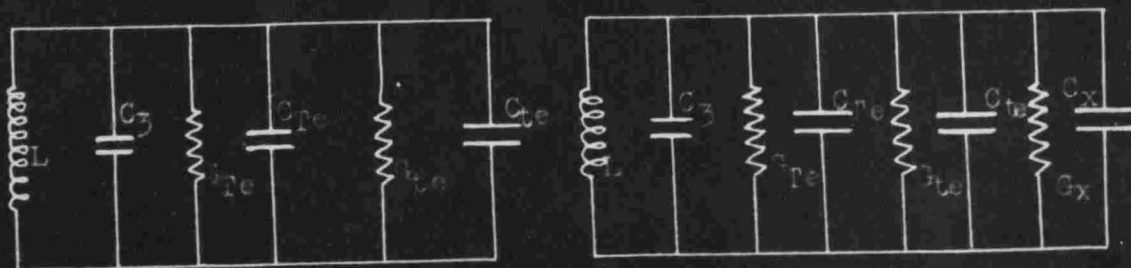
Expansion of Diode Circuit Conductance Calibration

Fig. 51



Expansion of Diode Circuit Conductance Calibration

fig. 52



Residuals, Reactance Variation Method

fig. 53